



**QUEEN'S  
UNIVERSITY  
BELFAST**

## **Modelling the effectiveness of grass buffer strips in managing muddy floods under a changing climate**

Mullan, D., Vandaele, K., Boardman, J., Meneely, J., & Crossley, L. H. (2016). Modelling the effectiveness of grass buffer strips in managing muddy floods under a changing climate. *Geomorphology*, 270, 102-120.  
<https://doi.org/10.1016/j.geomorph.2016.07.012>

**Published in:**  
Geomorphology

**Document Version:**  
Peer reviewed version

**Queen's University Belfast - Research Portal:**  
[Link to publication record in Queen's University Belfast Research Portal](#)

### **Publisher rights**

© 2016 Elsevier B. V. This manuscript version is made available under the CC-BY-NC-ND 4.0 license  
<http://creativecommons.org/licenses/by-nc-nd/4.0/>, which permits distribution and reproduction for non-commercial purposes, provided the author and source are cited.

### **General rights**

Copyright for the publications made accessible via the Queen's University Belfast Research Portal is retained by the author(s) and / or other copyright owners and it is a condition of accessing these publications that users recognise and abide by the legal requirements associated with these rights.

### **Take down policy**

The Research Portal is Queen's institutional repository that provides access to Queen's research output. Every effort has been made to ensure that content in the Research Portal does not infringe any person's rights, or applicable UK laws. If you discover content in the Research Portal that you believe breaches copyright or violates any law, please contact [openaccess@qub.ac.uk](mailto:openaccess@qub.ac.uk).

# Modelling the effectiveness of grass buffer strips in managing muddy floods under a changing climate

\*Donal Mullan<sup>1</sup>, Karel Vandaele<sup>2</sup>, John Boardman<sup>3,4</sup>, John Meneely<sup>1</sup>, Laura Crossley<sup>5</sup>

<sup>1</sup> School of Geography, Archaeology and Palaeoecology, Queen's University Belfast, Belfast, Northern Ireland, UK

<sup>2</sup> Watering van Sint-Truiden, Sint-Truiden, Belgium

<sup>3</sup> Environmental Change Institute, Oxford University Centre for the Environment, University of Oxford, Oxford, England, UK

<sup>4</sup> Department of Environmental and Geographical Science, University of Cape Town, Rondebosch, South Africa.

<sup>5</sup> School of Geography and Environment, University of Southampton, Southampton, England, UK

\*Corresponding author e-mail [D.Mullan@qub.ac.uk](mailto:D.Mullan@qub.ac.uk); Tel: +44(0) 28 9097 3362

## Abstract

Muddy floods occur when rainfall generates runoff on agricultural land, detaching and transporting sediment into the surrounding natural and built environment. In the Belgian Loess Belt, muddy floods occur regularly and lead to considerable economic costs associated with damage to property and infrastructure. Mitigation measures designed to manage the problem have been tested in a pilot area within Flanders and were found to be cost-effective within three years. This study assesses whether these mitigation measures will remain effective under a changing climate. To test this, the Water Erosion Prediction Project (WEPP) model was used to examine muddy flooding diagnostics (precipitation, runoff, soil loss and sediment yield) for a case study hillslope in Flanders where grass buffer strips are currently used as a mitigation measure. The model was run for present day conditions and then under 33 future site-specific climate scenarios. These future scenarios were generated from three earth system models driven by four representative concentration pathways and downscaled using quantile mapping and the weather generator CLIGEN. Results reveal that under the majority of future scenarios, muddy flooding diagnostics are projected to increase, mostly as a consequence of large scale precipitation events rather than mean changes. The magnitude of muddy flood events for a given return period is also generally projected to increase. These findings indicate that present day mitigation measures may have a reduced capacity to manage muddy flooding given the changes imposed by a warming climate with an enhanced hydrological cycle. Revisions to the design of existing mitigation measures within existing policy frameworks is considered the most effective way to account for the impacts of climate change in future mitigation planning.

**Keywords:** muddy flooding; climate change; grass buffer strips; runoff; soil erosion; sediment yield.

## 1. Introduction

The 'off-site' impacts of soil erosion have become a major source of concern in recent decades due largely to the environmental damage and economic costs associated with 'muddy flooding' (Boardman, 2010). Muddy floods occur when high volumes of runoff are generated on agricultural land, initiating the detachment and transport of considerable quantities of soil as suspended sediment or bedload (Boardman et al., 2006). It is therefore a fluvial process rather than a form of mass movement, but is distinguished from riverine flooding because it originates in valleys without permanent watercourses in the form of runoff generated on hillslopes and in the thalweg following rainfall (Evrard et al., 2007a). Muddy floods are reported across the loess belt of western and central Europe (Boardman et al., 1994; Boardman et al., 2006; Boardman, 2010; Evrard et al., 2010). A principal cause of muddy flooding in the region is the switch from grassland to arable crops creating intermittently exposed bare land surfaces (Boardman, 2010). In Belgium and France, for example, muddy flooding is generally limited to late spring and early summer when crops such as maize, sugar beet, chicory and potatoes offer low resistance to runoff (Auzet et al., 2006; Verstraeten et al., 2006). In southern England and the Paris basin, muddy floods are associated with autumn and winter cereals (Boardman, 2010). The role of rainfall in triggering muddy floods is a second crucial factor, with spring-sown cereals susceptible to intense thunderstorm activity generating mainly Hortonian runoff, and winter cereals susceptible to both intense and prolonged rainfall generating Hortonian and saturation-excess runoff (Boardman, 2010). A third physical factor in causing muddy floods is the erodible nature of the loess soils in the region. The soils are highly susceptible to crusting (Evrard et al., 2008a). This reduces their infiltration capacity and surface roughness, promoting enhanced runoff. A final factor is the proximity to high density urban areas since, by definition, muddy flooding damages property and public infrastructure (Boardman, 2010). The costs associated with muddy flooding demonstrate why it has become a considerable socio-economic issue in recent decades across the European loess belt. There are few extensive calculations of mean annual costs, but several examples of costs related to specific muddy flooding events. For example, muddy floods led to a mean damage cost of €118 ha<sup>-1</sup> y<sup>-1</sup> in the village of Soucy, France (Evrard et al., 2010), while damages at four sites in the suburbs of Brighton, England were estimated at €957,000 (Robinson and Blackman, 1990). The most extensive calculation of costs come from Belgium, where the mean annual cost

to private householders is estimated at €1.6-16.5 million, while the damage to public infrastructure is estimated at €12.5-122 million (Evrard et al., 2007b).

Given the high costs associated with muddy flooding, mitigation measures have been adopted across parts of the European loess belt to control the extent of the damage. One type of mitigation is to implement alternative farming practices to address the issue at the source, with the sowing of cover crops and adoption of conservation tillage examples of these measures (Gyssels et al., 2002; Leys et al., 2007). The implementation of these practices depend on the willingness of the farmer, and for this reason they have not been widely adopted across Europe (Holland, 2004). Much more common are measures aimed at buffering, rerouting or storing runoff in order to protect the areas impacted by muddy floods. Grass buffer strips and grassed waterways act to slow runoff, increase infiltration and decrease net soil loss (Le Bissonnais et al., 2004), while retention ponds are constructed to store runoff and reduce peak discharges in downstream areas (Evrard et al., 2007b). The main obstacle to the widespread uptake of these mitigation measures is typically the lack of national-level policy (Boardman and Vandaele, 2010). An exception to this is the 'Erosion decree,' established by the Flemish government in 2001, providing subsidies to farmers for mitigation measures (Verstraeten et al., 2003). Within this framework, an erosion mitigation scheme was drawn up at the catchment scale and piloted for the 200 km<sup>2</sup> Melsterbeek catchment. Between 2002 and 2005, 120 grass buffer strips and grassed waterways were installed, and 35 earthen dams constructed (Evrard et al., 2008a). Within the catchment, a pilot thalweg draining to Velm village was extensively monitored between 2005 and 2007 following the installation of a 12 ha grassed waterway and three earthen dams in the preceding three years (Evrard et al., 2007b; 2008b). Peak discharge was reduced by 69%, runoff coefficients decreased by 50% and sediment yield decreased by 93% between the head and outlet of the catchment (Evrard et al., 2008b). Furthermore, the mitigation measures were found to be cost-effective within three years, with a cost of €126 ha<sup>-1</sup> for control measures for a 20 year period compared to the mean damage cost associated with muddy floods in the area (€54 ha<sup>-1</sup> y<sup>-1</sup>) (Evrard et al., 2008b).

The success of these measures may diminish over the coming decades, however, as climate change poses new threats ranging from direct changes in rainfall characteristics to the indirect effects of changing land use and farming practices

(Pruski and Nearing, 2002a). Several studies have modelled the impacts of climate change on soil erosion, for example in Austria (Klik and Eitzinger, 2010); Brazil (Favis-Mortlock and Guerra, 1999; 2000); China (Zhang and Liu, 2005; Zhang, 2007; Zhang et al., 2009); England (Boardman et al., 1990; Boardman and Favis-Mortlock, 1993; Favis-Mortlock and Boardman, 1995; Favis-Mortlock and Savabi, 1996); Northern Ireland (Favis-Mortlock and Mullan, 2011; Mullan et al., 2012a; Mullan, 2013a, 2013b); and USA (Phillips et al., 1993; Lee et al., 1996; Nearing, 2001; Pruski and Nearing, 2002a, 2002b; Nearing et al., 2004, 2005; Zhang et al., 2004; O'Neal et al., 2005; Zhang, 2005; Zhang and Nearing, 2005). These studies typically employ a soil erosion model – most commonly the Water Erosion Prediction Project (WEPP) (Flanagan and Nearing, 1995) – in conjunction with climate scenarios derived from general circulation models and applied as change factors or in more recent studies downscaled for site-specific impact assessment (e.g., Zhang et al., 2004; Zhang, 2005; Zhang and Lui, 2005; Zhang, 2007; Zhang et al., 2009; Favis-Mortlock and Mullan, 2011; Mullan et al., 2012a Mullan, 2013a, b). A smaller selection of studies have also factored in changes in land use and management (e.g., O'Neal et al., 2005; Favis-Mortlock and Mullan, 2011; Mullan et al., 2012a; Mullan, 2013a, 2013 b). While some of these studies have modelled future soil erosion rates in the context of the off-site impacts, no study to date has examined explicitly changes in muddy flooding or the effects of climate change on mitigation measures designed to reduce muddy flooding. The aim of this study is to model the impacts of climate change (temperature and precipitation) on muddy flooding for a case study hillslope where mitigation measures have been implemented within the 200 km<sup>2</sup> Melsterbeek catchment in Flanders, Belgium. Given the success of present-day mitigation measures, the key research question seeks to address if these mitigation measures will continue to be successful in a changing climate. In terms of scientific significance, these results will build on the existing studies that have examined climate change impacts on soil erosion. These studies are important in assisting with conservation planning. Employing the widely used WEPP model alongside the use of downscaling techniques based on the latest state-of-the-art Earth System Models (ESMs) represents an advance on many previous climate change-soil erosion studies. The study is also vital in a more local context since local water authorities, land use managers, farmers and local residents will all be impacted by any changes in muddy flooding that threaten to compromise existing mitigation measures. In particular, results will be disseminated to the local water authority

responsible for managing muddy flooding in the Limburg province so they can help influence decision-making on future mitigation planning.

## **2. Materials and Methods**

### **2.1 Study area**

The Belgian loess belt is a *ca.* 9000 km<sup>2</sup> plateau with a mean altitude of 115 m gently sloping to the north (Fig. 1). Belgium has a temperate maritime climate influenced by the North Sea and Atlantic Ocean with cool summers and mild winters. The mean annual temperature is 9-10°C with a mean annual precipitation range of 700-900 mm (Hufty, 2001). The rainfall distribution is relatively even throughout the year, with a slight peak in rainfall erosivity between May and September (Verstraeten et al., 2006). Soils are mostly loess-derived haplic luvisols (World Reference Base, 1998). Arable land dominates the Belgian loess belt, covering around 65% of the land surface in the area (Statistics Belgium, 2006). The dominant crops are cereal, industrial and fodder crops such as sugar beet, oilseed rape, maize, chicory and potatoes. These summer crops have largely replaced winter cereals in the past few decades (Evrard et al., 2007a). Farmers are encouraged to sow cover crops such as mustard and phacelia during the dormant late spring and early summer period while summer crops establish sufficient cover to protect the soil (Biielders et al., 2003).

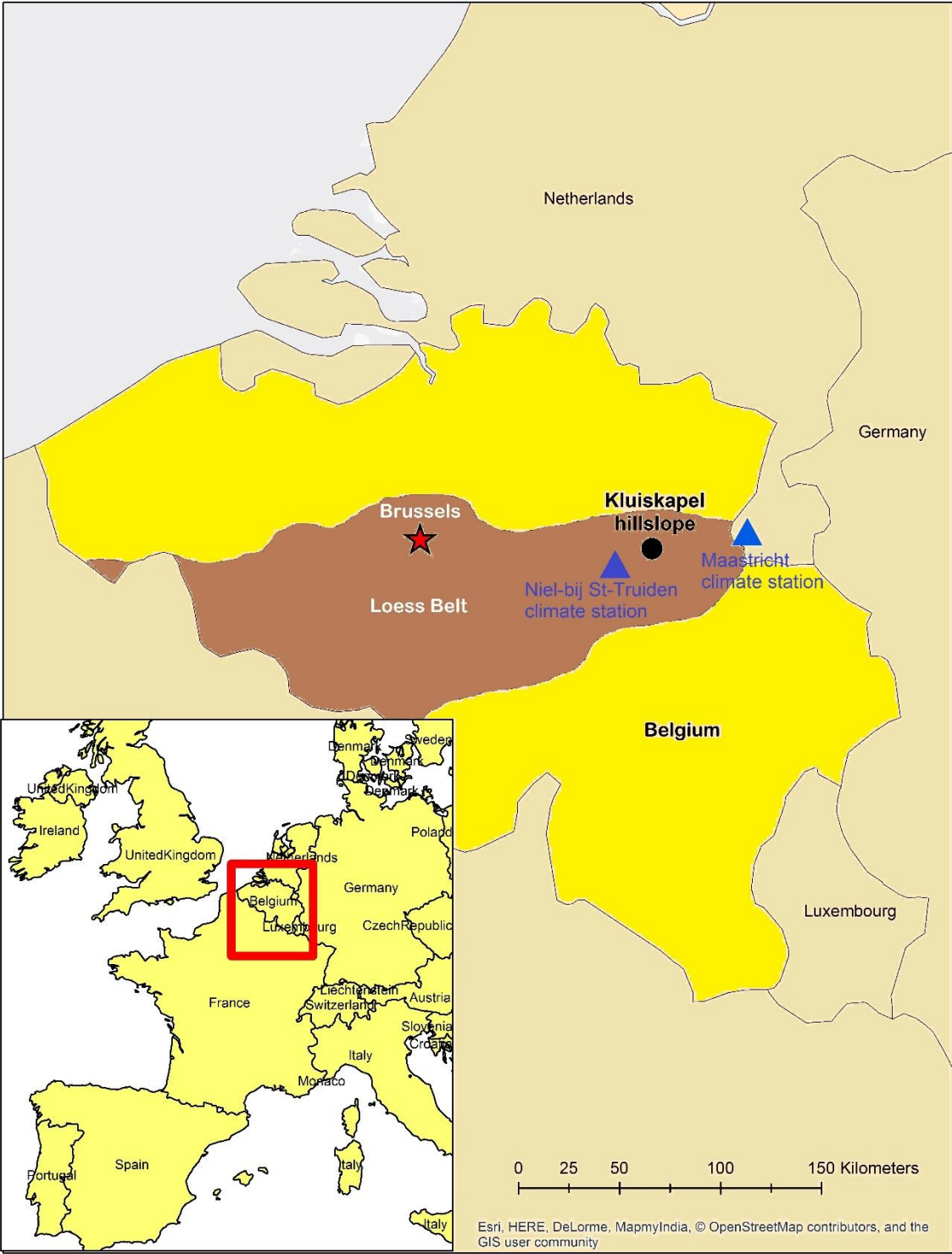


**Fig. 1.** The study area.

The case study site, herein referred to as Kluiskapel hillslope, is a 340 m long hillslope within a 7.3 ha field located in the 200 km<sup>2</sup> Melsterbeek catchment near the town of St-Truiden in the Flanders region of Belgium. The area has been affected by numerous muddy floods in the past couple of decades, with a local water agency



tasked specifically with installing and maintaining mitigation measures (Evrard et al., 2007b). The elevation within the slope ranges between 80 and 95 m.a.s.l. As determined from a 10 m resolution digital elevation model (described further in section 2.3), the slope is broadly convex in the upper half and concave in the lower half, with an average steepness of 4.2% (Fig. 2).



**Fig. 2.** Variation of slope angles within Kluiskapel hillslope.

As determined by laboratory testing of soil samples as described in section 2.3, the soil type is very typical of the European loess belt. It is a silty loam with 81% silt content and 4.5% organic matter. The long-term mean annual temperature, taken from the nearby station in Maastricht in the Netherlands (described further in section 2.3), is 10°C, and the mean annual precipitation is 769 mm, with the season occurring in the summer wettest. Fig. 3 shows how long-term temperatures and precipitation have changed at Maastricht. Temperatures have clearly risen in recent decades, while precipitation has fluctuated considerably. A typical crop rotation involves maize, followed by soybeans, with a cover crop of grass sown in both years. Tillage normally



occurs early in spring, with a finer seed bed established some six weeks later before planting. Crops are typically harvested in mid-autumn.

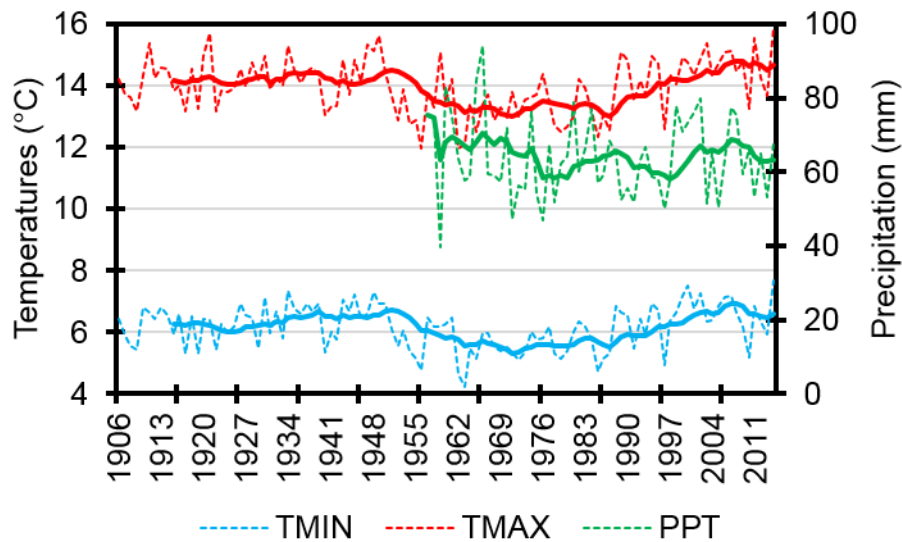


**Fig. 3.** Changes in temperatures (1906-2014) and precipitation (1906-2014) at Maastricht.

## 2.2 The WEPP model

The Water Erosion Prediction Project (WEPP) model (Flanagan and Nearing, 1995) (v.2008.907) was selected to simulate muddy flooding diagnostics (runoff, soil loss, deposition and sediment yield) under observed and future climatic conditions. WEPP is a physically-based, continuous simulation model that simulates hydrology, water balance, plant growth, soil and erosion at field, hillslope and watershed scales. WEPP was selected because it is the most commonly used model for climate change-soil erosion studies (see introduction) and is used here to simulate ‘present-day’ and future rates of muddy flooding at Kluiskapel hillslope. WEPP requires four input parameter files representing slope, soil, land management, and climate. These four input files are described with respect to how they were parameterised in the subsequent section.

Climate data in WEPP is simulated using the weather generator CLIGEN (Nicks et al., 1995). CLIGEN produces long sequences of synthetic weather data based on the statistical properties of the observed climate. In order to construct daily sequences of climate data, CLIGEN requires monthly means and standard deviations for maximum and minimum temperature and solar radiation; monthly mean, standard deviation and skewness for wind speed; and monthly mean wind direction % split into

16 compass directions. The most important climatic input variables are those relating to precipitation. CLIGEN requires monthly means, standard deviations and skewness values for mean precipitation per wet day. Also required to calculate sequences of wet and dry days are the transitional probabilities of a wet day following a wet day ( $P_{w/w}$ ) and a wet day following a dry day ( $P_{w/d}$ ). Finally, monthly maximum half hour precipitation values (MX.5P) and time to peak rainfall intensity values (Time Pk) are required to calculate rainfall intensity. These values are all calculated on a monthly basis with the exception of the 12 Time Pk values. Instead, the Time Pk values describe an empirical probability distribution of the time to peak rainfall intensity as a fraction of storm duration (Yu, 2003). The full list of CLIGEN input parameters is shown in Table 1.

	Parameter	Unit	1	2	3	4	5	6	7	8	9	10	11	12
1	Mean P	in	Mean daily precipitation per wet day for each month											
2	SD P	in	Standard deviation of Mean P per month											
3	Skew P	in	Skewness of Mean P per month											
4	$P_{w/w}$	%	Probability of a wet day following a wet day for each month											
5	$P_{w/d}$	%	Probability of a wet day following a dry day for each month											
6	TMAX AV	°F	Mean maximum temperature for each month											
7	TMIN AV	°F	Mean minimum temperature for each month											
8	SD TMAX	°F	Standard deviation of TMAX AV per month											
9	SD TMIN	°F	Standard deviation of TMIN AV per month											
10	SOL.RAD	L/d*	Mean solar radiation for each month											
11	SD SOL	L/d*	Standard deviation of SOL.RAD per month											
12	MX.5P	in	Mean maximum half hourly precipitation for each month											
13	DEW PT	°F	Mean dew point temperature for each month											
14	Time Pk	**	Time to peak rainfall intensity											
15	% DIR***	%	Mean % wind from 1 of 16 compass directions for each month											
16	MEAN	m/s <sup>-1</sup>	Mean wind speed associated with % DIR per month											
17	SD	m/s <sup>-1</sup>	Standard deviation of MEAN per month											
18	SKEW	m/s <sup>-1</sup>	Skewness of MEAN per month											
19	CALM	%	Mean % of days with mean wind speed < 1 ms <sup>-1</sup> per month											

**Table 1.** Input parameters required to run the weather generator CLIGEN.

\*L/d = Langleys/day.

\*\*For all parameters except 14, columns 1-19 represent calendar months.

\*\*\*% DIR refers to 16 different compass directions for wind direction. These are N, NNE, NE, ENE, E, ESE, SE, SSE, S, SSW, SW, WSW, W, WNW, NW, NNW. Lines 15-18 therefore appear 16 times in a CLIGEN parameter file, meaning there are a total of 948 input values to CLIGEN (79 lines x 12).

## 2.3 Parameterising WEPP for the observed period

A slope profile for Kluiskapel hillslope was developed by extracting length and elevation data from a 10 m resolution digital elevation model (DEM) based on airborne

laser scanning for the area. Although a higher resolution DEM would be preferable, Zhang et al. (2008) demonstrated that a 10 m LiDAR-derived DEM created realistic field boundaries, stream networks and hillslopes, and actually compared more closely to observed runoff and erosion rates across two small forested catchments in the USA. These results built on earlier work by Zhang and Montgomery (1994) also indicating that a 10m resolution DEM achieved an appropriate balance between necessary topographic accuracy and computation. For the soils file, bulk soil samples to a 15 cm depth were extracted using a soil auger. Five 15-cm deep samples were extracted per sampling location (15 cm x 5 = total depth of 75 cm) at 18 sampling locations evenly distributed between the top and bottom of the slope, generating a total of 90 soil samples. These were then analysed in the laboratory with respect to soil texture and organic matter (OM). Effective hydraulic conductivity, critical shear, and erodibility values were calculated using equations from the WEPP user manual (Flanagan and Livingston, 1995). The soil properties are shown in Table 2. Plant growth parameters for the necessary crops were taken directly from the WEPP plant database (Flanagan and Nearing, 1995). The selected crops for modelling were maize one year and soybeans the next, as this represents a typical crop rotation for this hillslope. Dates for management operations were obtained directly from the farmer. The management file was split into two sections along two different overland flow elements (OFEs) of the same hillslope. The management file for the upper majority of the slope was parameterised as described above, while the bottom 21 m of the slope was parameterised as a strip of permanent grass, with values taken from the WEPP database to represent this land cover. This section of land management represents the 21 m grass buffer strip planted at the base of the Kluiskapel hillslope to act as a mitigation measure for muddy floods from the slope. The key details of the management files in WEPP are shown in Table 3.

Depth (cm)	Clay %	Silt %	Sand %	OM %	Kr (s/m)	Ki (kg s/m <sup>4</sup> )	Tc (n/m <sup>2</sup> )	Kb (mm h <sup>-1</sup> )	Albedo
0-15	11.2	80.5	8.3	4.5	0.021	5434397	3.5	1.62	0.10
16-30	10.9	79.9	9.1	4.2	0.022	5450501	3.5	1.70	0.11
31-45	10.5	80.8	8.7	4.2	0.023	5475242	3.5	1.66	0.11
46-60	10.5	81.2	8.3	4.8	0.023	5477699	3.5	1.63	0.09
61-75	10.2	80.9	8.8	4.8	0.024	5489447	3.5	1.67	0.09
Mean	10.7	80.7	8.6	4.5	0.023	5465457	3.5	1.66	0.10

**Table 2.** Measured and estimated input parameters representing soil conditions at Kluiskapel hillslope. Kr = rill erodibility; Ki = interrill erodibility; Tc = baseline critical flow hydraulic shear; baseline effective hydraulic conductivity.

Year	Operation	Crop	Management Dates
1	Initial conditions	Ryegrass cover crop	1 Jan
	Tillage	Chisel Plow 30 cm depth	1 Mar
	Tillage	Harrow-roller 5 cm depth	15 Apr
	Plant	Corn (maize) – medium fertilisation	15 Apr
	Harvest	Corn (maize) – medium fertilisation	15 Oct
	Tillage	Chisel Plow 30 cm depth	15 Oct
	Plant	Ryegrass – medium fertilisation	15 Oct
2	Tillage	Chisel Plow 30 cm depth	1 Mar
	Tillage	Harrow-roller 5 cm depth	15 Apr
	Plant	Soybeans – medium fertilisation	15 Apr
	Harvest	Soybeans – medium fertilisation	15 Oct
	Tillage	Chisel Plow 30 cm depth	15 Oct
	Plant	Ryegrass – medium fertilisation	15 Oct

**Table 3.** Management details for Kluiskapel hillslope.

Climate data was obtained from the Royal Netherlands Meteorological Institute (KNMI) Climate Explorer site, which archives a range of freely available climate datasets. All climate data apart from sub-hourly precipitation were taken from Maastricht, The Netherlands and is shown in Table 4. No long-term climate datasets of good quality existed for St-Truiden or other stations in the east of Belgium, which is why the search was extended to the westerly part of The Netherlands. Maastricht is just 29 km from Kluiskapel hillslope as the crow flies, and with no major changes in topography or distance from the coast, it could be expected that both areas have very similar climates. Daily series of maximum and minimum temperature, wind speed and direction, and relative humidity from 1906-2014; precipitation from 1957-2014; and solar radiation from 1965-2014 were all extracted. The relative humidity data was converted to dew point temperature using Equation 1 (Alduchov and Eskridge, 1996).

**Equation 1.**

$$TD = 243.04 \left( \ln \left( \frac{RH}{100} \right) + \left( \frac{17.625 * T}{243.04 + T} \right) \right) / \left( 17.625 - \ln \left( \frac{RH}{100} \right) - \left( \frac{17.625 * T}{243.04 + T} \right) \right)$$

where TD = dew point temperature, RH = relative humidity; and T = mean temperature.

Finally, sub-hourly precipitation data from 2004-2014 was taken from Niel-bij-St-Truiden (13 km as the crow flies from Kluiskapel hillslope) rather than Maastricht in order to calculate MX.5P and Time Pk.

Variable downloaded	Temporal Resolution	Time Period	Converted?	CLIGEN variables applied to
Maximum Temperature	Daily	1906-2014	No	TMAX AV; SD TMAX
Minimum Temperature	Daily	1906-2014	No	TMIN AV; SD TMIN
Precipitation	Daily	1957-2014	No	Mean P; SD P; Skew P; P (W/W); P (W/D)
Solar Radiation	Sub-hourly*	1957-2014	No	MX.5P; Time Pk
Relative Humidity	Daily	1965-2014	No	SOL.RAD; SD SOL
	Daily	1906-2014	to Daily Dew Point Temperature using Equation 1	DEW PT
Wind Speed	Daily	1906-2014	No	MEAN; SD; SKEW; CALM
Wind Direction	Daily	1906-2014	No	% DIR

**Table 4.** Details on climate data downloaded for Maastricht climate station, as used to parameterise CLIGEN.

\*Sub-hourly precipitation data from Niel-bij-St-Truiden rather than Maastricht.

CLIGEN was run for 60 years in order to drive WEPP for a 60-year simulation representing present-day baseline conditions. This duration was chosen to allow for 30 cycles of the maize-soybeans two year crop rotation. In addition, a 1000-year CLIGEN file was generated to drive a 1000-year WEPP simulation representative of observed present-day conditions in order to facilitate the validation assessment (detailed in section 2.6).

## 2.4 Parameterising WEPP under a changed climate

### 2.4.1 Datasets required for downscaling

Climatic conditions in CLIGEN were perturbed based on future climate scenarios downscaled from three earth system models (ESMs) driven by four different representative concentration pathways (RCPs). ESMs are the current state-of-the-art models for simulating the global climate, and they expand on AOGCMs (atmosphere-ocean general circulation models) to include representation of various biogeochemical cycles including those in the carbon cycle, sulphur cycle or ozone (Flato, 2011). They

are the most comprehensive tools currently available for modelling the response of the climate system to past and future external forcing (Flato et al., 2013). In this study, three ESMs were selected in order to characterise some of the uncertainty associated with selecting a single model. The selected ESMs (Table 5) all participated in the Climate Model Intercomparison Project (CMIP5) – models which have been used to develop the scenarios and model evaluations for the Intergovernmental Panel on Climate Change (IPCC) Fifth Assessment Report (AR5) (Stocker et al., 2013). The three ESMs span almost the full range of equilibrium climate sensitivity (temperature change to doubling of atmospheric CO<sub>2</sub>) and transient climate response (change in temperature for 1% y<sup>-1</sup> increase in CO<sub>2</sub>) (Table 5) and thus represent a broad range of potential climate futures. The RCPs replace the Special Report on Emissions Scenarios (SRES) (Nakicenovic and Swart, 2000) used to drive climate model experiments in the IPCC Fourth Assessment Report. The four most commonly used RCPs are employed here, representing four contrasting pathways of radiative forcing up to the end of the 21<sup>st</sup> century, ranging from 2.6 W/m<sup>2</sup> to 8.5 W/m<sup>2</sup> (van Vuuren et al., 2011). These radiative forcing figures are a consequence of collaboration between integrated assessment modellers, climate modellers, terrestrial ecosystem modellers and emissions inventory experts. Details on the four RCPs used here are given in Table 6.

ESM	Organisation	Country	Spatial Resolution (°lat x °long)	Time Period	ECS °C	TCR °C	Key reference
GFDL-ESM2G	Geophysical Fluid Dynamics Laboratory	USA	2.0 x 2.5	1861-2100	2.4	1.1	Dunne et al. (2013)
MIROC-ESM	Japan Agency for Marine-Earth Science and Technology, Atmosphere and Ocean Research Institute (The University of Tokyo) and National Institute for Environmental Studies	Japan	2.81 x 2.81	1850-2100	4.7	2.2	Watanabe et al. (2011)
MPI-ESM-MR	Max Planck Institute for Meteorology	Germany	1.88 x 1.88	1850-2100	3.6	2.0	Stevens et al. (2013)

**Table 5.** Details on the ESMs used in this study.

RCP	Description	Key references
2.6	Peak in RF at ~3 W/m <sup>2</sup> (~490 ppm CO <sub>2</sub> eq) before 2100 and then decline to 2.6 W/m <sup>2</sup> by 2100	Van Vuuren et al. 2006, 2007
4.5	Stabilisation without overshoot pathway to 4.5 W/m <sup>2</sup> (~650 ppm CO <sub>2</sub> eq) at stabilisation after 2100	Smith and Wrigley 2006; Clarke et al. 2007; Wise et al. 2009)
6.0	Stabilisation without overshoot pathway to 6 W/m <sup>2</sup> (~850 ppm CO <sub>2</sub> eq) at stabilisation after 2100	Fujino et al. 2006; Hijioka et al. 2008)
8.5	Rising RF pathway leading to 8.5 W/m <sup>2</sup> (~1370 ppm CO <sub>2</sub> eq) by 2100	Riahi et al. 2007

**Table 6.** Details of the RCPs driving the selected ESMs in this study.

Monthly maximum and minimum temperature and monthly precipitation were downloaded from each ESM and RCP for the grid box overlying the target climate station at Maastricht. Observed daily series for the same climatic variables for Maastricht climate station as shown in Table 4 were aggregated to monthly series in order to facilitate the subsequent downscaling analysis.

#### **2.4.2 Spatial downscaling**

The downscaling approach used in this study is similar to the Generator for Point Climate Change (GPCC) method (Zhang, 2005; 2013; Zhang et al., 2012; Chen et al., 2014; Mullan et al., 2016). It is a two step approach first involving spatial downscaling of monthly climate scenarios from ESM grid box scale to site-specific climate station scale, followed by temporal downscaling from monthly to daily scenarios in order to enable CLIGEN to be perturbed to represent future conditions. As shown in Table 4, observed precipitation data for Maastricht spans the period 1957-2014 and observed temperature data runs from 1906-2014. Spatial downscaling was carried out using quantile mapping to bias correct the ESM data. For each calendar month, the ranked observational monthly TMAX, TMIN or PPT (y-axis) was plotted against the ranked quantiles of the ESM series (x-axis) using QQ-plots. A univariate linear function was



fit to each plot to construct transfer functions on a monthly basis. Polynomial fits were also tested but found to offer no improvement.

The calibrated transfer functions were then fit to the entire period of the ESM data to create spatially downscaled series for the future period. The spatially downscaled series from the three ESMs and four RCPs were subdivided into four 20-year time slices: a hindcast period from 1986-2005 enabling comparison of future periods to a historical reference period; and three future time slices from 2016-2035, 2046-2065 and 2081-2100. These are the same 20-year time slices used in the IPCC AR5. In theory, this would create 12 hindcast reference periods (3 ESMs x 4 RCPs) and 36 future climate scenarios (3 ESMs x 4 RCPs x 3 future time slices). In fact, the actual number is 11 hindcast periods and 33 future scenarios because one of the ESMs (MPI) had no data available under RCP6.

To test model performance, the probability distributions of the downscaled series were compared with the observed monthly series for the period of overlap. In order to test if the linear functions are suitable under nonstationary climate conditions, the observed and ESM data were split into two equal periods – with the first half of the record used to develop transfer functions and the second half used as a validation period to compare fitted probability distributions to the observed series.

### **2.4.3 Temporal Downscaling**

Temporal downscaling from monthly series to daily series necessary for WEPP simulation was achieved through the weather generator CLIGEN. In theory, any of the 948 input values in Table 1 could be modified to represent changed climatic conditions in CLIGEN. In this study, maximum and minimum temperature and precipitation were the modified climatic variables, with other parameters left unchanged.

Spatially downscaled means of TMAX and TMIN were directly used in CLIGEN as the adjusted monthly means for each future modelled scenario. Standard deviations for TMAX and TMIN were obtained using Equation 2 following Zhang et al. (2004).

#### **Equation 2.**

$$SDdESM = (SDdOBS)(\Delta SDmESM)$$

where  $SD_{dESM}$  = daily standard deviation for future TMAX and TMIN;  $SD_{dOBS}$  = daily standard deviation for the observed baseline; and  $\Delta SD_{mESM}$  = change in the monthly standard deviation between the future time slice and the hindcast period of each ESM.

With respect to precipitation, there are further decisions to be made about how to modify precipitation related parameters. In this study, the precipitation intensity parameter Time Pk and skewness of precipitation were left unchanged as there is no straightforward way to modify these parameters. Mean P, SD P, the transitional probabilities of wet and dry day sequences, and MX.5P were the parameters that were modified in this study. The transitional probabilities were calculated by establishing linear relationships between transitional probabilities and mean daily precipitation for the observed period on a monthly basis. Transfer functions were then forced with mean daily precipitation for the future period to calculate changed transitional probabilities. In order to preserve the projected mean monthly precipitation totals ( $R_m$ ) following the adjustment of transitional probabilities, Mean P was calculated using the approach of Zhang et al. (2004, 2012). First, the unconditional probability of precipitation occurrence ( $\pi$ ) is calculated as follows:

**Equation 3.**

$$\pi = \frac{P_w/d}{1 + \frac{P_w}{d} - P_w/d}$$

The new Mean P is then calculated using:

**Equation 4.**

$$Mean P = \frac{R_m}{N_d \pi}$$

where Mean P and  $R_m$  are as described before,  $N_d$  is the number of days in the month and  $N_d \pi$  is the expected number of wet days in the month.

Changes in SD P were calculated in exactly the same manner as was used for temperature in Equation 2. MX.5P changes were calculated based on the study of Zhang (2016), where linear relationships were developed between relative changes in MX.5P ( $R_{MX.5P}$ ) and relative changes in mean monthly precipitation ( $R_{MMP}$ ) for 23 sites across the USA. The relative changes were calculated by splitting the daily data from each station into two equal halves.  $R_{MX.5P}$  and  $R_{MMP}$  were then calculated for each half and calendar month to fit the model:

**Equation 5.**

$$\frac{\Delta R_{MX.5P}}{R_{MX.5P}} = \beta \frac{\Delta R_{MMP}}{R_{MMP}}$$

where  $\Delta$  is the differential changes between the two halves and  $\beta$  is the slope of a linear regression without an intercept.

In Zhang (2016), Equation 5 was fit to 12 data points at each station (one per month) and to all 23 stations and a regression equation developed. In this study, the regression equation for these 23 sites was then forced with the ratio of  $\Delta R_{MMP}$  between the hindcast and future periods of each future scenario to  $R_{MMP}$  (i.e., the right hand side of Equation 5).

## **2.5 Running WEPP under a changed climate**

WEPP was run for the future by holding the slope and soil input files constant from the present-day simulation and perturbing the climate file under the various downscaled climate scenarios. As with the baseline period, 60-year CLIGEN files representing future climate scenarios were created in order to drive 60-year WEPP simulations. For each of these future scenarios, the planting and harvest dates in the management file were also modified. This was done by calculating the change in the number of growing days between the observed period and each future scenario and then delaying the planting dates by half that amount and bringing harvest forward by the other half. For example, if a future climate scenario projected 10 more growing days in the future, then planting would be delayed by five days and harvest brought forward by five days. In the few cases where there were more than 60 extra growing days projected per

year, the planting dates and harvest dates were not moved by more than one month in either direction as the growing season would be unrealistically short if dates were moved beyond this. A similar approach to modifying management dates has been used in Zhang et al. (2004, 2012) and Mullan et al. (2012a) and Mullan (2013a, 2013b). A total of 33 future scenarios were simulated, representing three ESMs x four RCPs x three future time slices, minus one unavailable ESM-RCP combination for each future time slice.

Future muddy flooding diagnostics outputted by WEPP include mean annual precipitation (MAP), mean annual runoff (MAR), mean annual soil loss (MASL) and mean annual sediment yield (MASY). Other analysed outputs include mean maximum monthly precipitation (MXP) and calculated return periods for MAP, MAR, MASL and MASY.

## **2.6 Model Validation**

WEPP was validated for Kluiskapel hillslope under present-day conditions using volumetric calculations of deposited sediment following a muddy flood event in summer 2014 at the site.

### **2.6.1 The Event**

The muddy flood event occurred on 29 July 2014 after an intense thunderstorm that affected much of Limburg province. The storm was highly spatially heterogeneous, with daily rainfall amounts between zero and 80 mm across Limburg. The exact amount and intensity of the rainfall event precisely at Kluiskapel hillslope on 29 July 2014 is unknown as there is not a rain gauge at the field site, but local weather observations recorded daily rainfall amounts between 31 mm and 80 mm at nearby stations. Moreover, it is highly likely the daily rainfall amount lies somewhere between 43 mm and 80 mm as these amounts were recorded by the two nearest rain gauges – both within 2 km of the field site on either side. The rainfall event caused rilling within the hillslope, resulting in the deposition of sediment in five distinct depositional zones within the grass buffer strip at the base of Kluiskapel hillslope (Fig. 4).

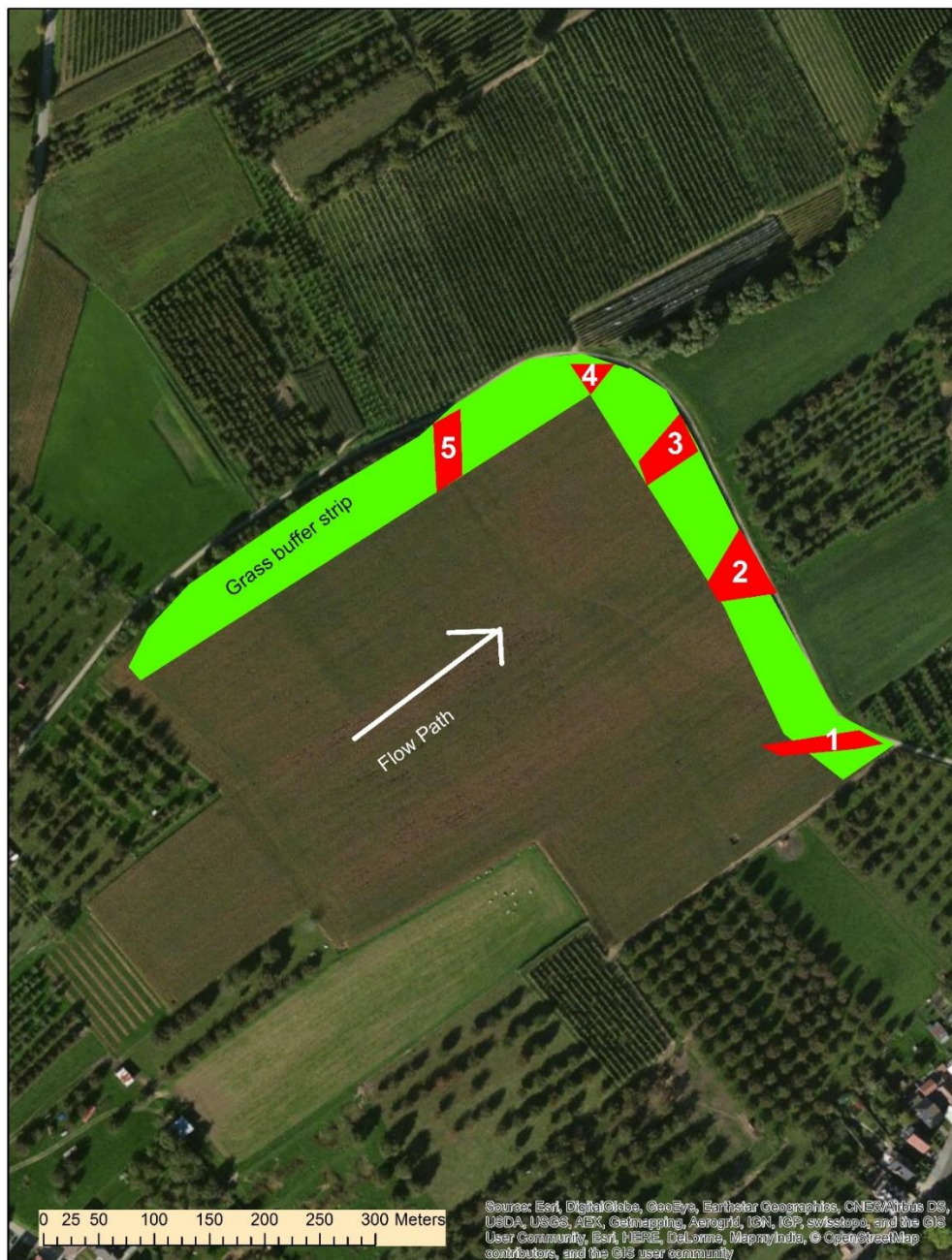


**Fig. 4.** Sedimentation zones (1-5) at Kluiskapel hillslope after the muddy flood event described above.

### **2.6.2 Sedimentation Calculations**

The volume of sediment was calculated for each sedimentation zone and added to obtain a figure of total sediment deposited. The volumetric calculation was converted to  $t\ ha^{-1}$  to facilitate comparison with simulated soil loss using Equation 6.

**Equation 6.**

$$S_{Dep} = \left( \frac{VD}{CA} \right) * BD * 10,000$$

where  $S_{Dep}$  = sediment deposited ( $t\ ha^{-1}$ );  $VD$  = volume sediment deposited ( $m^3$ );  $CA$  = contributing area ( $m^2$ ); and  $BD$  = bulk density ( $t\ m^3$ ).

$VD$  was calculated by multiplying the cross-sectional depositional area ( $m^2$ ) by the length of deposition ( $m$ ).  $CA$  is simply the slope width ( $m$ ) x slope length ( $m$ ). The  $BD$  value was taken from Goidts and van Wesemael (2007) as a mean  $BD$  value for cropland in the Belgian loess belt. Applied to this study, Equation 6 is solved below:

**Equation 7.**

$$S_{Dep} = \left( \frac{90}{105,400} \right) * 1.4 * 10,000$$

**2.6.3 Measured vs Simulated Events**

A selection of soil loss events from the 1000-year present day WEPP output from Kluiskapel hillslope was extracted according to those events most similar to the measured event. In this respect, those events simulated from May-August inclusive were first extracted. Then, two different ranges were extracted. First, Validation Criteria 1 (VC1) consisted of a wider range encompassing all soil loss events with associated rainfall amounts between 31 mm and 80 mm and regardless of storm duration (i.e., the full range of rainfall amounts recorded at nearby stations on the day of the event). Validation Criteria 2 (VC2) employed a narrower range encompassing all soil loss events with rainfall amounts between 43 mm and 80 mm whose storm duration is two hours or less (i.e., the reported rainfall characteristics from the two nearest rain gauges on the day of the event). In both cases, a linear relationship between rainfall amount and soil loss for these simulated events was developed and used to predict soil loss for an event with rainfall amounts in the range of the measured events.

513

## 514 **3 Results**

515

### 516 **3.1 Model Validation**

517         The storm on 29 July 2014 at Kluiskapel hillslope resulted in a sedimentation  
518 zone measuring 90 m<sup>3</sup>. This translates to 12 t ha<sup>-1</sup>. This figure compares reasonably  
519 closely to the WEPP simulated mean annual soil loss rate of 16.5 t ha<sup>-1</sup>, but as shown  
520 in Fig. 5 there is a considerable degree of scatter for the simulated soil loss rate during  
521 events.

522



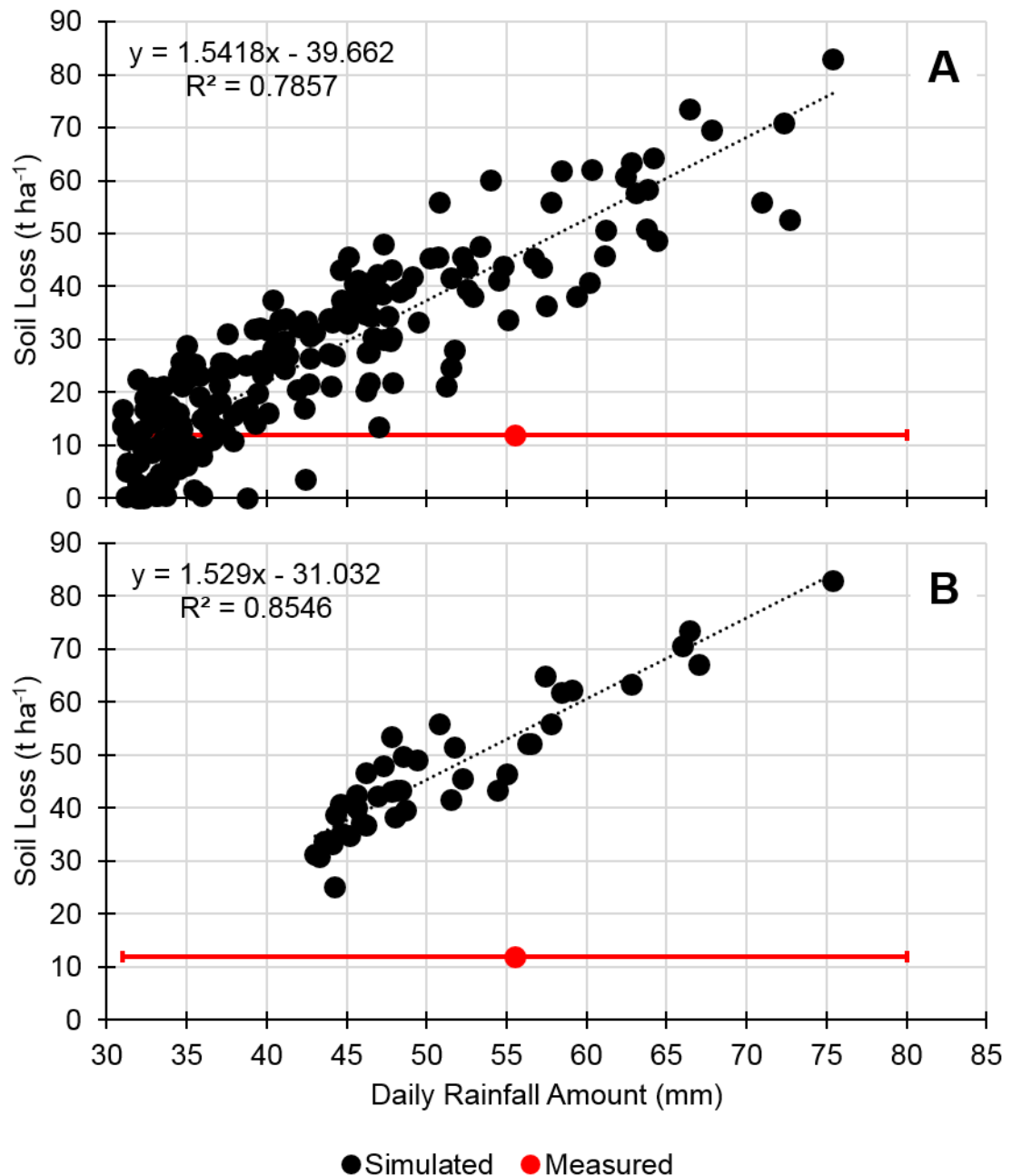


**Fig. 5.** Daily simulated rainfall amount vs simulated soil loss events based on a) VC1; and b) V2, and their comparison to the measured validation event.

The full simulated range of soil loss rates during events between 31 mm and 80 mm (i.e., VC1) is 0-84 t ha<sup>-1</sup>. Of the 544 simulated events corresponding to VC1 (Fig. 5a), 74% lie above the measured soil loss rate and 26% fall below it. When considering the full rainfall range in this manner, it is difficult to establish how well WEPP simulates soil loss at Kluiskapel hillslope as the range encompasses the measured rate and large amounts both below and above it. To illustrate the extreme

difference between a rainfall event of 31 mm and 80 mm, return periods were calculated based on 115 years of daily rainfall data from Maastricht climate station. This reveals a return period of 0.7 years for a rainfall amount of 31 mm and a return period of 115 years for a rainfall amount of 80 mm (i.e., it has only happened once in the 115-year record from Maastricht). When the narrower range of events simulated within VC2 is considered (Fig. 5b), the soil loss range changes to 25-83 t ha<sup>-1</sup>, with all 42 simulated events lying above the measured soil loss rate. Although the magnitude of the range is very similar to VC1, we can state that when VC2 is considered, WEPP is overpredicting soil loss rates for Kluiskapel hillslope, by a minimum of double the measured rate. This could relate to the hillslope length simulated. It has been found that WEPP tends to overpredict soil loss rates on slopes greater than 100 m long (Favis-Mortlock and Mullan, 2011). At 340 m long, the slope in this study therefore greatly exceeds this and may be vulnerable to overprediction. Nonetheless, WEPP has been applied to similar length slopes across Northern Ireland with soil loss rates that validate closely against measurements (e.g., Mullan, 2013a).

This comparison requires two points of caution. First, the sedimentation zone cannot be compared directly with the simulated soil loss from WEPP. It is likely that not all soil lost would be deposited in the sedimentation zone as some may be redeposited within the field and some finer material may be lost beyond the sedimentation zone. Therefore, the measured amount should be lower than the simulated amount. Second, the measured muddy flood is a single event that may not be representative of long-term conditions. As shown in Fig. 5, there is considerable variation in the simulated response of soil loss to rainfall events of a very similar magnitude, which is something we also see in measured data (Nearing, 1998). This lack of long-term measured data at Kluiskapel hillslope is a considerable caveat to the current study, so results must be interpreted with this in mind. Greater confidence in the simulated rates of soil loss and sediment yield can be obtained by considering soil erosion rates from past field studies across Belgium. Historic evidence from small catchments in central Belgium (0.2-210 ha<sup>-1</sup>) obtained mostly from augering thick alluvial deposits reveal soil loss rates ranging from 2.1-16.9 t ha<sup>-1</sup> yr<sup>-1</sup> (Verstraten et al., 2006). The simulated mean annual soil loss in this study, at 16.5 t ha<sup>-1</sup> yr<sup>-1</sup>, lies towards the upper end of this range. Contemporary measurements of soil loss in central Belgium from rilling (the main process of soil loss in the measured event at Kluiskapel hillslope) lie below the mean annual simulated rate of soil loss in this study.

Govers (1991) surveyed 86 winter wheat and bare soil fields for three winter periods between 1982 and 1985 and found a mean rill erosion rate of 3.6 t ha<sup>-1</sup> per winter period. Vandaele (1997) also surveyed rill erosion rates between 1989 and 1992 across three small agricultural catchments with sugar beet, potato and maize crops and obtained rates of 1.4-4.5 t ha<sup>-1</sup> yr<sup>-1</sup>. Although these rates lie well below the mean annual simulated soil loss in this study, additional soil loss from interrill erosion at Kluiskapel hillslope means simulated rates may not be vastly overpredicted. Govers and Poesen (1988) calculated the ratio of rill to interrill erosion from an upland field plot near Leuven and found that interrill erosion contributed about 22% to total erosion. All considered, WEPP is likely to be overpredicting soil loss rates for Kluiskapel hillslope, but the measured event and historic and contemporary field measurements from central Belgium offer some indication that simulated results may not be too far from reality.

### 3.2 Mean Annual Changes

Table 7 shows the absolute and relative changes in muddy flooding diagnostics across all future climate scenarios for the near, mid and 21<sup>st</sup> century, while Fig. 6 shows the full distribution of projected changes in the same diagnostics for Kluiskapel hillslope under the same scenarios.

Diagnostic	Baseline	Future Mean	% change	Future Range	% change
MAP (mm)	759	843	11	725 to 1094	-5 to 44
MAR (mm)	11.2	17.1	52	7.6 to 28.2	-32 to 152
MASL (t ha <sup>-1</sup> )	16.5	22.1	34	6.5 to 39.8	-61 to 141
MASY (t ha <sup>-1</sup> )	5.6	9.0	61	3.1 to 16.8	-45 to 200

**Table 7.** Present-day baseline and future simulated rates of muddy flooding diagnostics. % changes are relative to the baseline and the range is across all 33 future climate scenarios.

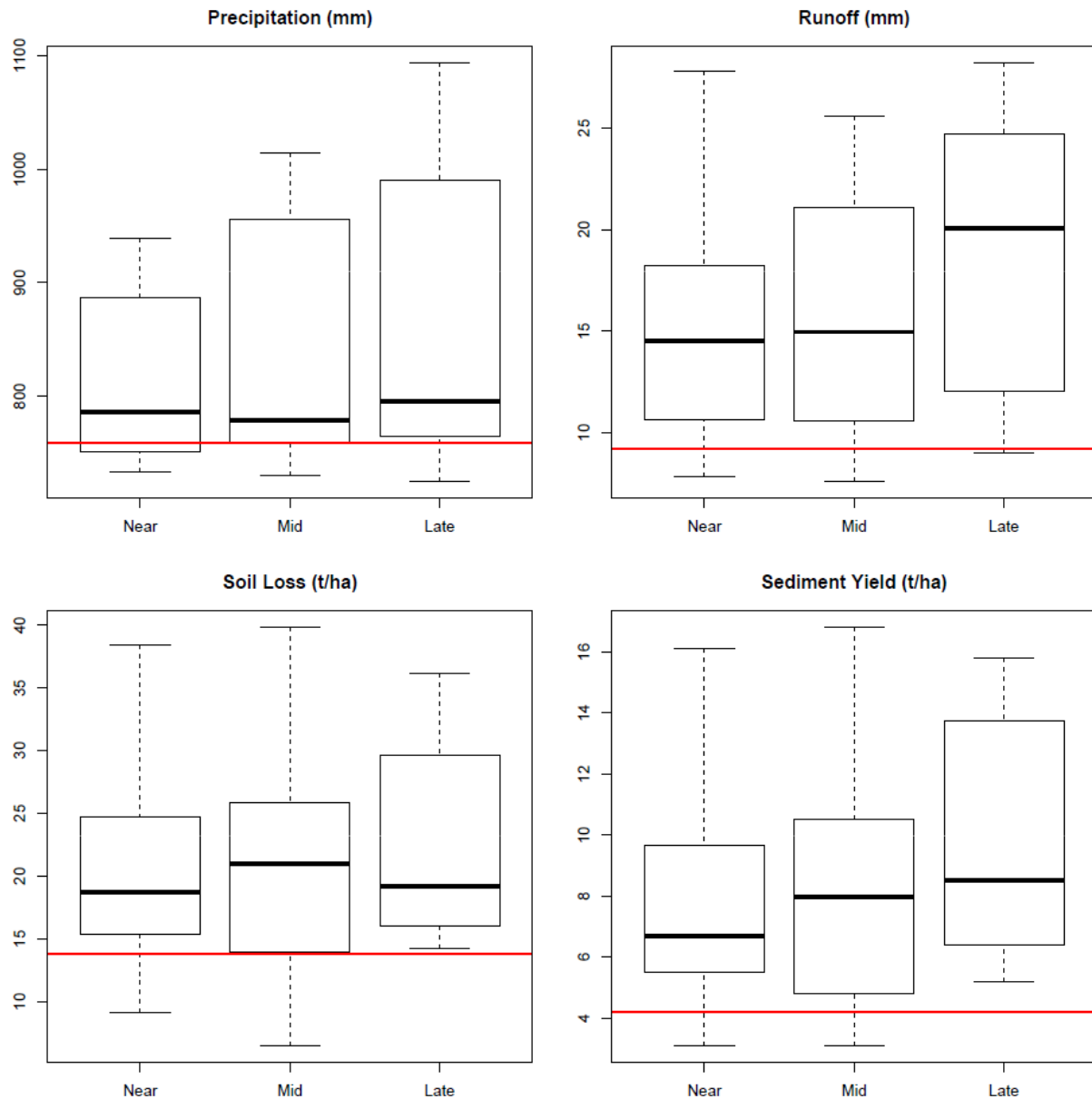


**Fig. 6.** Full distribution of all muddy flooding diagnostics across 33 future climate scenarios. Plotted in red is the present-day simulated value for each diagnostic.

All muddy flooding diagnostics are generally projected to increase throughout the 21<sup>st</sup> century. The median projected changes are higher than the observed baseline for all diagnostics and for all three future time slices. In addition, the 25<sup>th</sup> percentile exceeds the baseline for 10 out of 12 of the scenarios shown in Figure 6. The median projected changes for the near 21<sup>st</sup> century are 4% for MAP, 29% for MAR, 13% for MSL and 20% for MSY, with maximum changes of 24% for MAP, 148% for MAR, 133% for MSL and 188% for MSY. Four out of 11 scenarios project small decreases in MAP, with three for MAR, MSL and MSY. For the mid 21<sup>st</sup> century, median projected changes in MAP are lower than the near 21<sup>st</sup> century at 3%, while maximum projected changes

are higher at 34%. In contrast, the response in the other three muddy flooding diagnostics shows higher projected changes in the median and in many cases lower projected maximum changes. The median changes are 34% for MAR, 27% for MSL and 42% for MSY, with maximum changes of 129% for MAR, 141% for MSL and 200% for MSY. The amount of scenarios projecting decreases is generally lower than the near 21<sup>st</sup> century, with three out of 11 scenarios projecting small decreases for all diagnostics. For the late 21<sup>st</sup> century, median and maximum projected changes in muddy flooding diagnostics are generally at their highest. Median changes are 5% for MAP, 79% for MAR, 16% for MSL and 52% for MSY (highest of all time slices apart from MSL), while maximum changes are 44% for MAP, 152% for MAR, 119% for MSL and 182% for MSY. Just one out of 11 scenarios project small decreases for all muddy flooding diagnostics for the late 21<sup>st</sup> century.

### **3.3 Seasonal Changes**

In addition to the projected annual precipitation totals, the seasonal distribution of rainfall is critical in triggering muddy flood events. Figs. 7-9 show projected monthly distribution of sediment yield (SY) as well as mean monthly precipitation totals (MMP) and mean maximum monthly precipitation (MXP) for all ESM-RCP combinations for the near 21<sup>st</sup> century (Fig. 5), mid 21<sup>st</sup> century (Fig. 8) and late 21<sup>st</sup> century (Fig. 9). Also shown is the observed baseline in each case and the date when tillage and planting of maize one year and soybeans the next occurs (for the baseline management scenario). The key months of concern are late April-August following tillage and planting, as this time represents the critical phase of late spring and summer when the land surface is most exposed. A short period from mid-October to December is also a vulnerable time for the soil surface following harvesting.

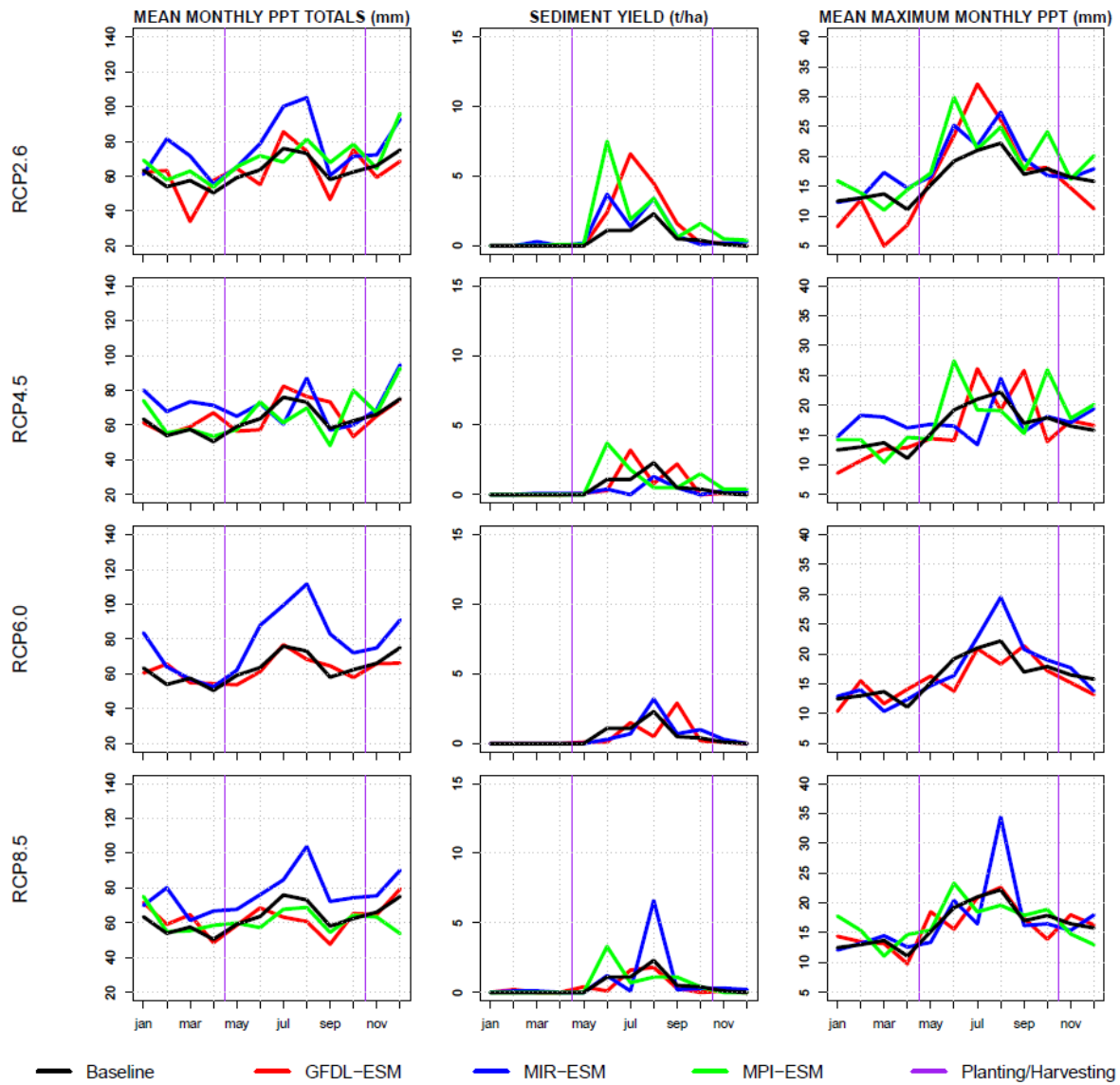


**Fig. 7.** Projected monthly distributions of SY, MMP and MXP for the present-day and under 11 future climate scenarios for the near 21<sup>st</sup> century. Also marked are the dates of key farming operations.

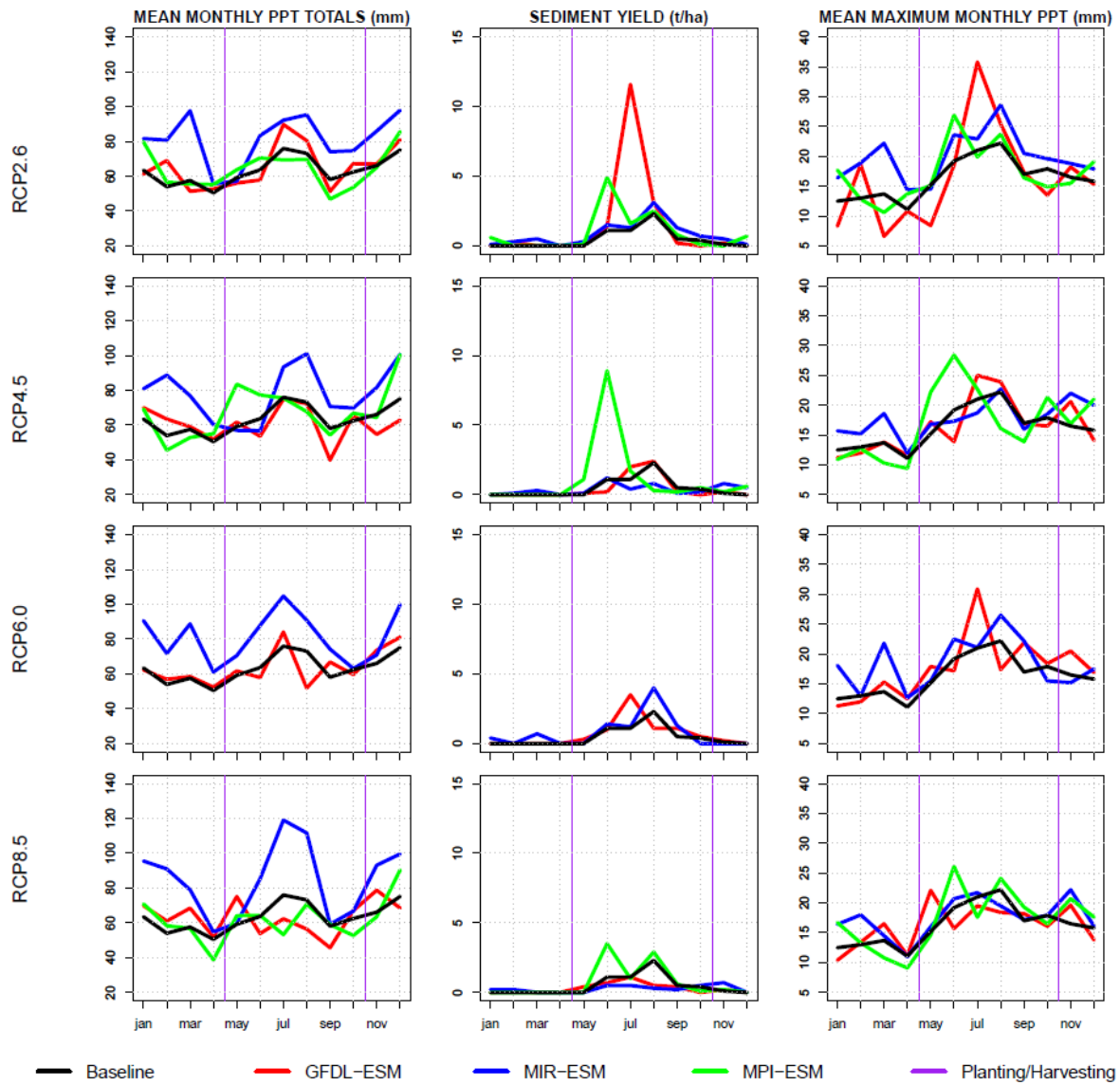


**Fig. 8.** Same as Fig. 7, but for the mid 21<sup>st</sup> century.



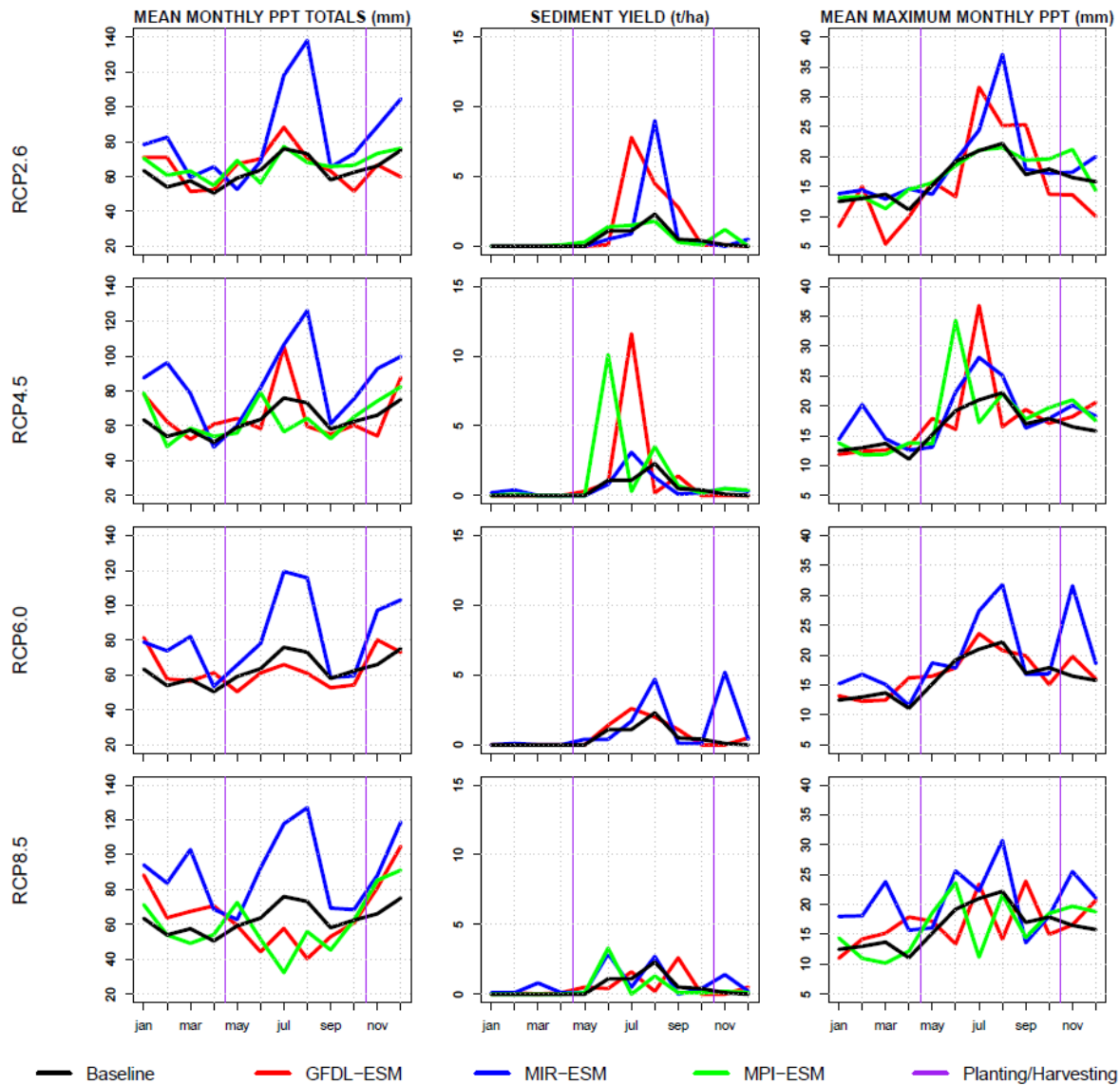


**Fig. 9.** Same as Fig. 7, but for the late 21<sup>st</sup> century.

MMP shows a mixture of projected increases and decreases from the observed baseline for all three future time slices during these key months. MIR-ESM stands out with the largest increases in MMP, particularly during the month of August. For example, MIR-ESM driven by RCP8.5 results in a doubling of MMP for the late 21<sup>st</sup> century (Fig. 9). For GFDL-ESM and MPI-ESM, it is much more of a mixed picture, with several scenarios projecting increases and decreases in MMP, sometimes even within the same summer season. As also shown in Figs. 7-9, projections of MXP are also very mixed across different scenarios. The changes in MXP do not necessarily correspond with changes in MMP, as there are several examples where one increases and the other decreases from the observed baseline. For example, during the month of July for the mid 21<sup>st</sup> century (Fig. 8), MMP is projected to increase by over 10%

under MIR-ESM driven by RCP4.5, while the corresponding scenario for MXP projects a decrease by over 10%. In contrast, one of the highest MXP values projected by any scenario for any time period is 36 mm by GFDL-ESM under RCP2.6 for the month of June for the mid 21<sup>st</sup> century (Fig. 8). Yet the corresponding scenario of MMP is only moderately higher than the observed baseline. Figs. 7-9 also show that SY corresponds much more closely to MXP than to MMP. For example, during the month of July for the mid 21<sup>st</sup> century (Fig. 8), GFDL-ESM driven by RCP2.6 projects a very large increase in SY (200%), yet the corresponding scenario for MAP projects only a very small increase. This is because the corresponding scenario for MXP projects a considerably larger increase of almost 50%. This clearly shows that changes in MXP rather than MMP are the chief cause of changes in SY.

In terms of changing seasonality, there is minimal change in the proportional distribution of all muddy flooding diagnostics between the baseline and future. For the three summer months where most muddy flooding occurs, the baseline proportion of muddy flooding diagnostics is 28% for MAP, 68% for MAR, 79% for MASL and 80% for MASY. As a mean of all 33 future scenarios, the proportions for the same months are 27% for MAP, 66% for MAR, 72% for MASL and 73% for MASY.

### 3.4 Changes in Return Periods

Figs. 10-12 show changes in return periods of total precipitation amounts and SY during muddy flooding events for the modelled baseline period as well as under the various ESM-RCP combinations for the near 21<sup>st</sup> century (Fig. 10), mid 21<sup>st</sup> century (Fig. 11) and late 21<sup>st</sup> century (Fig. 12). For all three future time slices, typically two out of the three ESMs project higher magnitude events for a given return period than the baseline. The largest change for PPT is projected by MPI-ESM driven by RCP4.5 for the late 21<sup>st</sup> century, where a 120-year return period has a magnitude of 132 mm for PPT, compared to the baseline PPT of 75 mm for the same return period. For SY, the 120-year return period for the same scenario has a magnitude of 93 t ha<sup>-1</sup>, compared to the baseline SY of 46 t ha<sup>-1</sup>.

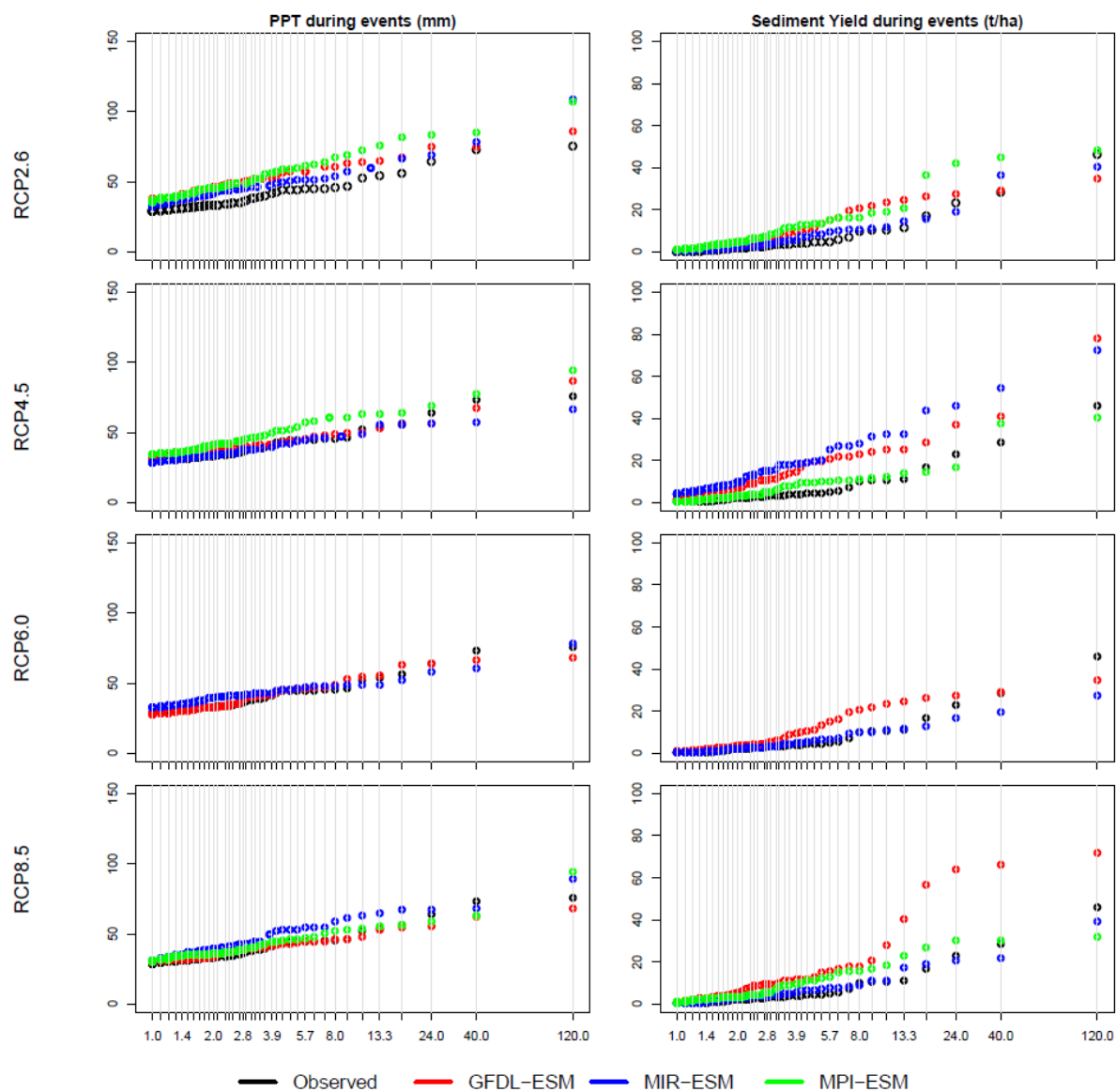


**Fig. 10.** Return Periods for PPT and SY for the present-day and under 11 future climate scenarios for the near 21<sup>st</sup> century.

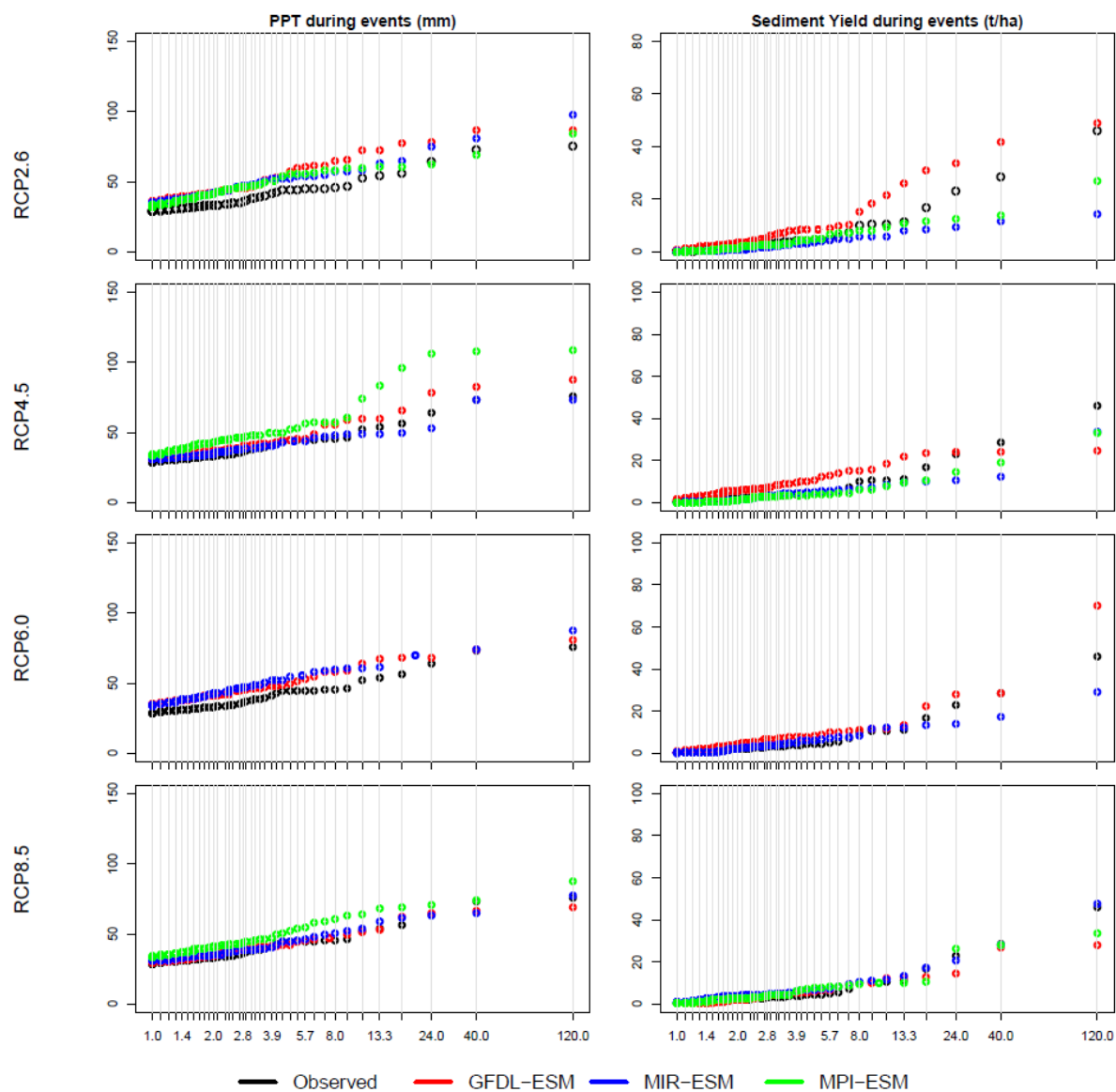


Fig. 11. Same as Fig. 10, but for the mid 21<sup>st</sup> century.

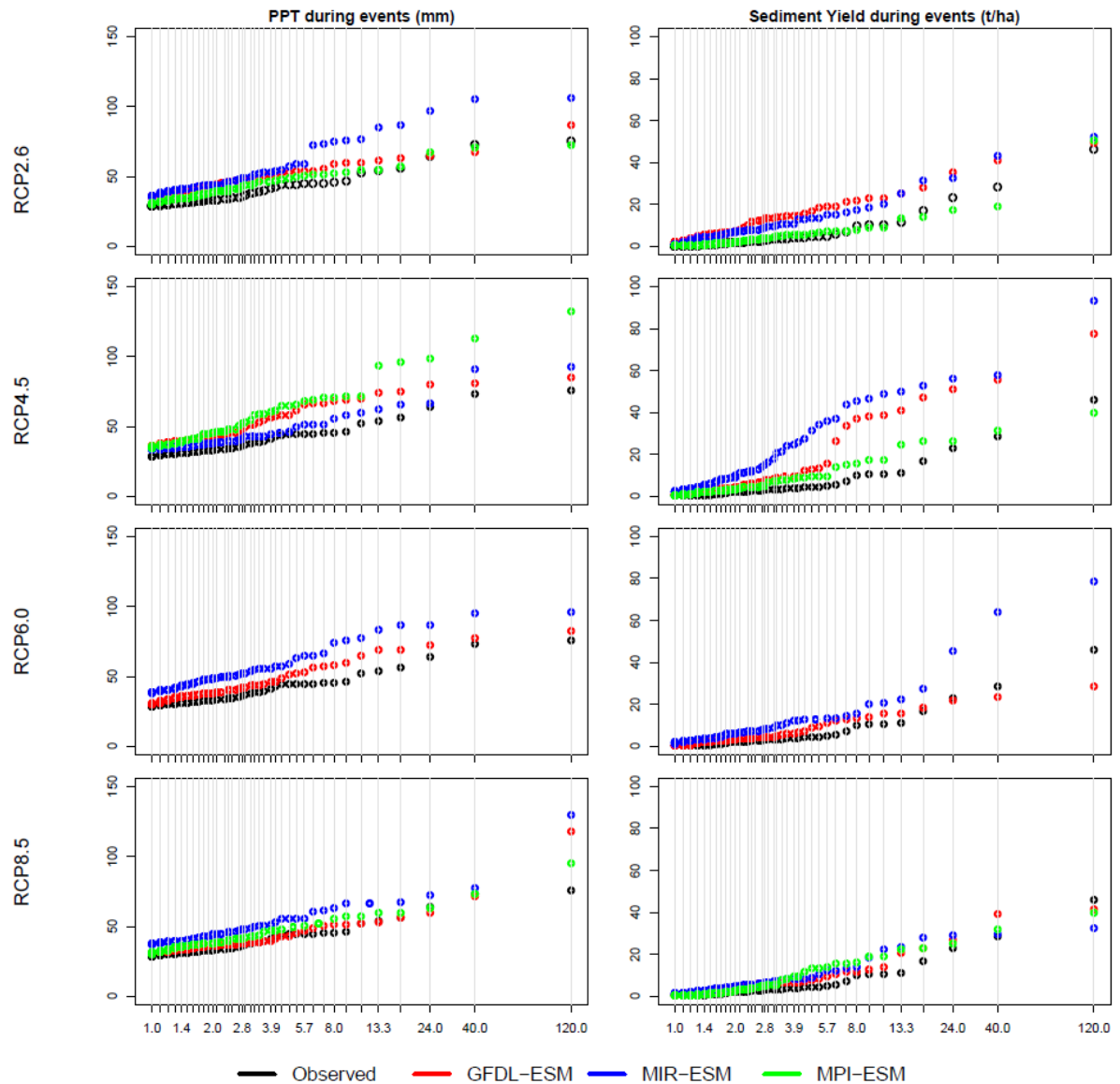


Fig. 12. Same as Fig. 10, but for the late 21<sup>st</sup> century.

## 4 Discussion

The results presented and described in section 3 reveal a wide range of potential changes in muddy flooding diagnostics at Kluiskapel hillslope, depending on which scenario is considered. This section discusses some of the key points and implications emerging from these findings.

### 4.1 Timing is everything

As shown in Figs. 7-9, muddy flood events will only occur when high mean monthly precipitation totals or intense precipitation events occur during the time of year when

the land surface is exposed. In the case study area and central Belgium generally, this is currently the late spring and early summer months between tillage and planting of crops such as maize and soybeans in mid-April and the time taken to establish a sufficient crop cover to protect the soil surface, typically around August. There is also a period in the late autumn from mid-October following harvesting when the land surface is vulnerable for around the *ca.* six weeks it takes for the cover crop to establish. For both the baseline period and all future scenarios, soil loss and sediment yield from Kluiskapel hillslope generally only occur during these key months. For the baseline period, no sediment yield occurs during the relatively less vulnerable months of January-May. As an average of all 33 future scenarios, this increases but remains low at just 5% for the same months, highlighting the role of timing with respect to farming operations in causing muddy floods. Specifically, the three summer months are when most of the damage occurs. For example, under MPI-ESM driven by RCP8.5 for the mid 21<sup>st</sup> century (Fig. 8), 90% of the sediment yield was generated during the three summer months despite these months not being the wettest projected months of the year. With 90 mm precipitation in December (the highest of the year), no sediment was lost from the hillslope. The timing of elevated rainfall amounts/intensity with inadequate crop cover is a well-established cause of soil erosion and muddy flooding and is also reported in many studies including Mullan et al. (2012a) and Mullan (2013a; b). For a more in-depth commentary on the role of timing with respect to rainfall and land cover in causing soil erosion, see Boardman and Favis-Mortlock (2014) and Burt et al. (2015).

## **4.2 Changes in extremes are key**

As shown in Figs. 7-9 and described in section 3.3, changes in MASL and MASY align much more closely with MXP than MAP. There are several instances in Figs. 7-9 where increases in MAP have not yielded consequent increases in MASY, even during the key vulnerable summer months. Just because MAP increases it does not necessarily mean precipitation amounts or intensities within individual storms increases. But in all cases where MXP increases, MASY responds with an increase. This illustrates that muddy flood events are typically driven by storms with high precipitation amounts and/or intensities rather than increases in monthly means that can mask the effects of individual storm events. Changes in extremes are further

illustrated in the changing return periods projected in Figs. 10-12. Muddy flood events of a given return period are typically projected to become higher in magnitude in a majority of scenarios. These results are in keeping with the literature for Flanders, which suggests that most muddy flood events are triggered by intense short-lived thunderstorms (Evrard et al., 2007b).

### **4.3 Choice of climate scenarios is critical**

In this study, three ESMs driven by four RCPs were used as the basis for projecting future changes in muddy flooding diagnostics. As Figs. 6-12 show, there is considerable variation between individual scenarios. Fig. 6 shows that the 11 scenarios for each of the three future time slices all include at least one scenario where each of the muddy flooding diagnostics decrease from the baseline period, but most of the future scenarios project an increase. The MIR-ESM tends to project the largest increases in MAP while the magnitude of changes in MXP and consequently MAR and MASY are relatively mixed between all models. The three selected ESMs were purposely selected to span a wide range of climate sensitivities, so the wide variation in the response of muddy flooding metrics is not surprising. As the model with the highest equilibrium climate sensitivity (ECS), it is not surprising that MIR-ESM projects the highest increases in precipitation due to the warmer atmosphere projected by this model, but it is rather more surprising that the ‘colder’ two models in certain scenarios project larger increases in intense precipitation events. Differences in precipitation projections, however, are caused by more than simply the enhancement of the hydrological cycle by additional heat in the atmosphere. The role of clouds in particular is very important in the modelling of precipitation, and it is well documented that cloud feedbacks are one of the chief causes of model errors with respect to the simulation of precipitation fields (Bony and Dufresne, 2005; Andrews et al., 2012). The simulation of precipitation is therefore more complex and non-linear than temperature and consequently results in a wide spread between scenarios. In this respect, although the model selection in this study spans a wide range of climate sensitivities that captures well the temperature range between CMIP5 models, this does not mean the selection captures the widest range of precipitation response between models. The use of a wider range of CMIP5 models would therefore be desirable in presenting a wider selection of scenarios of muddy flooding.



765

#### 766 **4.4 Uncertainty should not mean inaction**

767 Given the complexity of climate science and the large envelope of uncertainty around  
768 modelled projections, uncertainty has been flagged as one of the key arguments for  
769 delaying or avoiding action (Moser, 2010). With progress made in mitigating muddy  
770 floods in the present day following the adoption of the 2001 Erosion Decree, it is  
771 important that the impacts of a changing climate are factored into the mitigation  
772 process in a proactive way. The wide range of future scenarios presented here makes  
773 low-regret, flexible and 'soft solutions' most desirable as adaptation options (Wilby and  
774 Dessai, 2010). Grass buffer strips and grassed waterways in particular are good  
775 examples of such options in the sense that their dimensions can be modified relatively  
776 quickly and easily as the situation worsens over time. Given the results presented in  
777 this study, the characteristics (e.g., width, length, grass species, etc.) of these natural  
778 mitigation measures will need to be revised to accommodate increased runoff and  
779 sediment yield. More research is needed to examine how this can be best achieved to  
780 reduce the impacts of more frequent/intense muddy flood events in a way that  
781 balances this with the need to keep their dimensions minimal to avoid needless extra  
782 compensation to farmers. In terms of earthen dams and retention ponds, these are not  
783 as flexible as the buffer strips and waterways since they are designed to be effective  
784 for decades rather than from year to year. That said, they can be very effectively  
785 modified to account for the impacts of climate change by simply altering their  
786 dimensions and storage capacities with information on modelled return periods. Again,  
787 research is needed to provide specific information on modified characteristics of these  
788 'harder' mitigation measures. The benefit of the suggestions outlined above is that  
789 these measures have all been shown to be effective at managing muddy flooding in  
790 the present day, driven by existing policy structures. Small revisions to these existing  
791 measures seems the most sensible way to achieving continued success in mitigating  
792 muddy flooding under the impacts of a changing climate.

793

#### 794 **4.5 What do we still need to know?**

795 First, this study focused on the impacts of climate change on muddy flooding, but did  
796 not consider changes in land use and management. These changes have been shown  
797 to in many cases be a more significant factor in driving increases in soil erosion than

climate change (e.g., O'Neal et al., 2005; Mullan et al., 2012a; Mullan, 2013a, 2013b). Future studies should examine this crucial factor. Second, changes in sub-daily rainfall intensity are not considered here, given the lack of information available at this temporal resolution from climate models. Refining the temporal resolution of rainfall scenarios remains a key research requirement for the wider climate modelling community. Third, while this study has provided an indication of future rates of muddy flooding diagnostics for one hillslope in Flanders, it does not claim to be representative of conditions across the wider region. A larger project would need to be undertaken to project changes in muddy flooding diagnostics for more of the erosion hotspots across Flanders. Fourth, the study does not answer any questions on the spatial patterns of soil erosion and sediment yield from the case study hillslope or whether events are most largely generated from interrill, rill or gully erosion. Finally, it is imperative that further monitoring is conducted across pilot thalwegs and catchments within Flanders in order to construct databases that help more fully ascertain the present day extent of the problem as well as greatly assist in model construction and validation.

## **5 Conclusions and Implications**

Mitigation measures to manage muddy flooding in Flanders are cost-effective within three years. This study sought to investigate whether or not these mitigation measures would remain effective under a changing climate. In this respect, changes in muddy flooding diagnostics were modelled for a case study hillslope in Flanders under a variety of future climate scenarios. The key findings and implications are as follows:

- Present-day baseline sediment yield from Kluiskapel hillslope was projected at  $5.6 \text{ t ha}^{-1} \text{ yr}^{-1}$ . Based on calculations of a sedimentation zone following a muddy flood event in 2014, this projected rate fell within the measured range, though a refined measured range indicates that projections may be overestimated.
- Projected sediment yield as a mean of all 33 future climate scenarios is 61% higher than the baseline at  $9.0 \text{ t ha}^{-1} \text{ yr}^{-1}$ , with a majority of scenarios projecting increases in muddy flooding diagnostics.
- The magnitude of events of a given return period is generally projected to increase under a majority of future scenarios.

- Changes in sediment yield are governed more closely by large-scale precipitation events than changes in monthly means.
- Given the projected increases in muddy flooding diagnostics, present-day mitigation measures may not suffice in controlling the problem in the future. Current mitigation measures are working, but may need to be modified to account for the impacts of climate change.
- Uncertainty in modelled scenarios should not be used as an excuse for inaction. Mitigation measures based around low-cost, flexible and ‘soft’ solutions seem the most effective way of dealing with uncertainty in a proactive manner.
- This is most likely to involve changes in design capacities and dimensions of existing measures, which should be implemented through existing policy structures.

## Acknowledgments

We thank the British Society for Geomorphology for providing an early career grant to the lead author to help make this study possible.

## References

- Alduchov, O.A., Eskridge, R.E., 1996. Improved magnus form approximation of saturation vapor pressure. *J. Appl. Meteorol.* 35, 601-609.
- Andrews, T., Gregory, J.M., Webb, M.J., Taylor, K.E., 2012. Forcing, feedbacks and climate sensitivity in CMIP5 coupled atmosphere-ocean climate models. *Geophys. Res. Lett.* 39 (9), L09, 712, DOI: 10.1029/2012GL051607.
- Auzet, A-V., Le Bissonnais, Y., Souchère, V., 2006. France, in: Boardman, J., Poesen, J. (Eds.), *Soil Erosion in Europe*. Wiley, Chichester, pp. 369-383.
- Bielders, C.L., Ramelot, C., Persoons, E., 2003. Farmer perception of runoff and erosion and extent of flooding in the silt-loam belt of the Belgian Walloon Region. *Env. Sci Policy.* 6, 85-93.
- Boardman, J., 2010. A short history of muddy floods. *Land Degrad. Dev.* 21, 303-309.
- Boardman, J., Evans, R., Favis-Mortlock, D.T., Harris, T.M., 1990. Climate change and soil erosion on agricultural land in England and Wales. *Land Degrad. Rehab.* 2, 95-106.
- Boardman, J., Favis-Mortlock, D.T., 1993. Climate change and soil erosion in Britain. *The Geographical J.* 159 (2), 179-183.

865 Boardman, J., Favis-Mortlock, D.T., 2014. The significance of drilling date and crop  
866 cover with reference to soil erosion by water, with implications for mitigating  
867 erosion on agricultural land in South East England. *Soil Use Manage.* 30, 40-47.

868 Boardman, J., Ligneau, L., De Roo, A., Vandaele, K., 1994. Flooding of property by  
869 runoff from agricultural land in northwestern Europe. *Geomorphology.* 10, 183-  
870 196.

871 Boardman, J., Vandaele, K., 2010. Soil erosion, muddy floods and the need for  
872 institutional memory. *Area.* 42, 502-513.

873 Boardman, J., Verstraeten, G., Bielders, C., 2006. Muddy floods, in: Boardman, J.,  
874 Poesen, J. (Eds.), *Soil Erosion in Europe*. Wiley, Chichester, pp. 743-755.

875 Bony, S., Dufresne, J-L., 2005. Marine boundary layer clouds at the heart of tropical  
876 cloud feedback uncertainties in climate models. *Geophys. Res. Lett.* DOI:  
877 10.1029/2005GL023851.

878 Burt, T., Boardman, J., Foster, I., Howden, N., 2015. More rain, less soil: long-term  
879 changes in rainfall intensity with climate change. *Earth Surf. Processes Landforms.*  
880 DOI: 10.1002/esp.3868.

881 Chen, J., Zhang, X.C., Brissette, F.P., 2014. Assessing scale effects for statistically  
882 downscaling precipitation with GPCC model. *Int. J. Climatol.* 34, 708-727.

883 Clarke, L.E., Edmonds, J.A., Jacoby, H.D., Pitcher, H., Reilly, J.M., Richels, R., 2007.  
884 Scenarios of greenhouse gas emissions and atmospheric concentrations. Sub-  
885 report 2.1a of Synthesis and Assessment Product 2.1. Climate Change Science  
886 Program and the Subcommittee on Global Change Research, Washington D.C.

887 Dunne, J.P. et al., 2013. GFDL's ESM2 global coupled climate-carbon earth system  
888 models. Part II: carbon system formulation and baseline simulation characteristics.  
889 *J. Clim.* 26, 2247-2267.

890 Evrard, O., Bielders, C.L., Vandaele, K., van Wesemael, B., 2007b. Spatial and  
891 temporal variation of muddy floods in central Belgium, off-site impacts and  
892 potential control measures. *Catena.* 70, 443-454.

893 Evrard, O., Heitz, C., Liégeois, M., Boardman, J., Vandaele, K., Auzet, A-V., van  
894 Wesemael, B., 2010. A comparison of management approaches to control muddy  
895 floods in central Belgium, northern France and southern England. *Land Degrad.*  
896 *Dev.* 21, 1-14.

897 Evrard, O., Persoons, E., Vandaele, K., van Wesemael, B., 2007a. Effectiveness of  
898 erosion mitigation measures to prevent muddy floods: A case study in the Belgian  
899 loam belt. *Agric. Ecosys. Env.* 118, 149-158.

900 Evrard, O., Vandaele, K., Bielders, C., van Wesemael, B., 2008a. Seasonal evolution  
901 of runoff generation on agricultural land in the Belgian loess belt and implications  
902 for muddy flood triggering. *Earth Surf. Processes Landforms.* 33, 1285-1301.

903 Evrard, O., Vandaele, K., van Wesemael, B., Bielders, C.L., 2008b. A grassed  
904 waterway and earthen dams to control muddy floods from a cultivated catchment  
905 of the Belgian loess belt. *Geomorphology.* 100, 419-428.

906 Favis-Mortlock, D.T., Boardman, J., 1995. Nonlinear responses of soil erosion to  
907 climate change: a modelling study on the UK South Downs. *Catena.* 25, 365- 387.

908 Favis-Mortlock, D.T., Guerra, A.J.T., 1999. The implications of general circulation  
909 model estimates of rainfall for future erosion: a case study from Brazil. *Catena*. 37,  
910 329- 354.

911 Favis-Mortlock, D.T., Guerra, A.J.T., 2000. The influence of global greenhouse-gas  
912 emissions on future rates of soil erosion: a case study from Brazil using WEPP-  
913 CO<sub>2</sub>, in: Schmidt, J. (Ed.), *Soil Erosion: Application of Physically Based Models*.  
914 Springer-Verlag, Berlin, pp. 3-31.

915 Favis-Mortlock, D.T., Mullan, D.J., 2011. Soil erosion by water under future climate  
916 change, in: Shukla, M. (Ed.) *Soil hydrology, land use and agriculture: measurement and modelling*. CABI, Oxford, pp. 384-414.

917

918 Favis-Mortlock, D.T., Savabi, M.R., 1996. Shifts in rates and spatial distributions of  
919 soil erosion and deposition under climate change, in: Anderson, M.G., Brooks,  
920 S.M. (Eds.), *Advances in Hillslope Processes*. Wiley, Chicester, pp. 529-560.

921 Flanagan, D.C., Livingston, S.J., 1995. USDA - Water Erosion Prediction Project  
922 (WEPP) User Summary. West Lafayette, IN., USA. National Soil Erosion Research  
923 Laboratory, USDA - Agricultural Research Service.

924 Flanagan, D. C., Nearing, M.A., 1995. USDA - Water Erosion Prediction Project  
925 (WEPP) Hillslope Profile and Watershed Model Documentation. West Lafayette,  
926 IN., USA. National Soil Erosion Research Laboratory, USDA - Agricultural  
927 Research Service.

928 Flato, G.M., 2011. Earth system models: an overview. *Wiley Interdiscip. Rev. Clim.*  
929 *Change*. 2 (6), 783-800.

930 Flato, G.M. et al., 2013. Evaluation of climate models. *Climate change 2013: the*  
931 *physical science basis. Contribution of working group I to the fifth assessment*  
932 *report of the Intergovernmental Panel on Climate Change*. Cambridge University  
933 Press.

934 Fujino, J., Nair, R., Kainuma, M., Masui, T., Matsuoka, Y., 2006. Multigas mitigation  
935 analysis on stabilization scenarios using aim global model. *The Energy Journal*  
936 *Special issue*. 3, 343–354.

937 Goidts, E., van Wesemael, B., 2007. Regional assessment of soil organic carbon  
938 changes under agriculture in southern Belgium (1955-2005). *Geoderma*. 141 (3-  
939 4), 341-354.

940 Govers, G., 1991. Rill erosion on arable land in central Belgium: rates, controls and  
941 predictability. *Catena*. 18, 133-155.

942 Govers, G., Poesen, J., 1988. Assessment of the interrill and rill contributions to total  
943 soil loss from an upland field plot. *Geomorphology*. 1, 343-354.

944 Gyssels, G., Poesen, J., Nachtergaele, J., Govers, G., 2002. The impact of sowing  
945 density of small grains on rill and ephemeral gully erosion in concentrated flow  
946 zones. *Soil Tillage Res.* 64 (3-4), 189-201.

947 Hijjoka, Y., Matsuoka, Y., Nishimoto, H., Masui, T., Kainuma, M., 2008. Global GHG  
948 emission scenarios under GHG concentration stabilization targets. *J. Glob.*  
949 *Environ. Eng.* 13, 97–108.

950 Holland, J.M., 2004. The environmental consequences of adopting conservation  
951 tillage in Europe: reviewing the evidence. *Agric. Ecosys. Env.* 103 (1), 1-25.

952 Hufty, A., 2001. Introduction à la climatologie. De Broeck Université, Brussels (In  
953 French), 542 pp.

954 Klik, A., Eitzinger, J., 2010. Impact of climate change on soil erosion and the efficiency  
955 of soil conservation practices in Austria. *J. Agric. Sci.* 148, 529-541.

956 Le Bissonnais, Y., Lecomte, V., Cerdan, O., 2004. Grass strip effects on runoff and  
957 soil loss. *Agronomie*. 24, 129-136.

958 Leys, A., Govers, G., Gillijns, K., Poesen, J., 2007. Conservation tillage on loamy soils:  
959 explaining the variability in interrill runoff and erosion reduction. *Eur. J. Soil Sci.*  
960 58, 1425-1436.

961 Lee, J.L., Phillips, D.L., Dobson, R.F., 1996. Sensitivity of the US Corn belt to climate  
962 change and elevated CO<sub>2</sub>: II. Soil erosion and organic carbon. *Agric. Syst.* 52,  
963 503-521.

964 Moser, S.C., 2010. Communicating climate change: history, challenges, process and  
965 future directions. *Wiley Interdiscip. Rev. Clim. Change*. 1, 31-53.

966 Mullan, D.J., 2013a. Soil erosion on agricultural land in the north of Ireland: past,  
967 present and future potential. *Irish Geography*. 45, 154-171.

968 Mullan, D.J., 2013b. Soil erosion under the impacts of future climate change:  
969 assessing the statistical significance of future changes and the potential on-site  
970 and off-site problems. *Catena*. 109, 234-246.

971 Mullan, D.J., Chen, J., Zhang, X.C., 2016. Validation of non-stationary precipitation  
972 series for site-specific impact assessment: comparison of two statistical  
973 downscaling techniques. *Clim. Dyn.* 46 (3), 967-986.

974 Mullan, D.J., Favis-Mortlock, D.T., Fealy, R., 2012a. Addressing key limitations  
975 associated with modelling soil erosion under the impacts of future climate  
976 change. *Agric. For. Meteorol.* 156, 18-30.

977 Mullan, D.J., Fealy, R., Favis-Mortlock, D.T., 2012b. Developing site-specific future  
978 temperature scenarios for Northern Ireland: Addressing key issues employing a  
979 statistical downscaling approach. *Int. J. Climatol.* 32 (13), 2007-2009.

980 Nakicenovic, N., Swart, R. (Eds.), 2000. Special Report on Emissions Scenarios. A  
981 Special Report of Working Group III of the Intergovernmental Panel on Climate  
982 Change. Cambridge University Press, Cambridge and New York.

983 Nearing, M.A., 1998. Why soil erosion models overpredict small soil losses and  
984 underpredict large soil losses. *Catena*. 32, 15-22. Nearing, M.A., 2001., Potential  
985 changes in rainfall erosivity in the U.S. with climate change during the 21<sup>st</sup> century.  
986 *J. Soil Water Conserv.* 56 (3), 229-232.

987 Nearing, M.A., Jetten, V., Baffaut, C., Cerdan, O., Couturier, A., Hernandez, M., Le  
988 Bissonnais, Y., Nichols, M.H., Nunes, J.P., Renschler, C.S., Souchère, V., van  
989 Oost, K., 2005. Modeling response of soil erosion and runoff to changes in  
990 precipitation and cover. *Catena*. 61, 131-154.

991 Nearing, M.A., Pruski, F.F., O'Neal, M.R., 2004. Expected climate change impacts on  
992 soil erosion rates: A Review. *J. Soil Water Conserv.* 59 (1), 43-50.

993 Nicks, A.D., Lane, L.J., Gander, G.A., 1995. Weather Generator, in: Flanagan, D.C.,  
994 Nearing, M.A. (Eds.), Hillslope profile and watershed model documentation.

995 NSERL Report no. 10, 2.1-2.2. West Lafayette, IN., USA: USDA-ARS National Soil  
996 Erosion Research Laboratory.

997 O'Neal, M.R., Nearing, M.A., Vining, R.C., Southworth, J., Pfeifer, R.A., 2005. Climate  
998 change impacts on soil erosion in Midwest United States with changes in crop  
999 management. *Catena*. 61, 165-184.

1000 Phillips, D.L., White, D., Johnson, C.B., 1993. Implications of climate change scenarios  
1001 for soil erosion potential in the USA. *Land Degrad. Rehab.* 4, 61-72.

1002 Pruski, F.F., Nearing, M.A., 2002a. Climate-induced changes in erosion during the 21<sup>st</sup>  
1003 century for eight U.S. locations. *Water Resour. Res.*, 38 (12), Article no. 1298.

1004 Pruski, F.F., Nearing, M.A., 2002b. Runoff and soil loss responses to changes in  
1005 precipitation: a computer simulation study. *J. Soil Water Conserv.* 57 (1), 7-16.

1006 Riahi, K., Grübler, A., Nakicenovic, N., 2007. Scenarios of long-term socio-economic  
1007 and environmental development under climate stabilization. *Technol. Forecast.*  
1008 *Soc. Change*. 74, 887–935.

1009 Robinson, D.A., Blackman, J.D., 1990. Some costs and consequences of soil erosion  
1010 and flooding around Brighton and Hove, autumn 1987, in: Boardman, J., Foster,  
1011 I.D.L., Dearing, J.A. (Eds.), *Soil Erosion on Agricultural Land*. Wiley, Chichester,  
1012 pp. 369-382.

1013 Smith, S.J., Wigley, T.M.L., 2006. MultiGas forcing stabilization with minicam. *The*  
1014 *Energy Journal Special issue*. 3, 373–392.

1015 Statistics Belgium, 2006. <http://www.statbel.fgov.be>.

1016 Stevens, B., Giorgetta, M., Esch, M., Mauritsen, T., Crueger, T., Rast, S., Salzmann,  
1017 M., Schmidt, H., Bader, J., Block, K., Brokopf, R., Fast, I., Kinne, S., Kornblueh,  
1018 L., Lohmann, L., Pincus, R., Reichler, T., Roeckner, E., 2013. Atmospheric  
1019 component of the MPI-M Earth System Model: ECHAM6. *J. Adv. Mod. Earth Sys.*  
1020 5 (2), 146-172.

1021 Stocker, T.F. et al., 2013. IPCC 2013: climate change 2013: the physical science  
1022 basis. Contribution of working group I to the fifth assessment report of the  
1023 Intergovernmental Panel on Climate Change. Cambridge University Press.

1024 Vandaele, K., 1997. Temporele en ruimtelijke dynamiek van bodemerrosieprocessen  
1025 in landelijke stroomgebieden (Midden-België); een terreinstudie. Unpublished PhD  
1026 Thesis, Faculty of Sciences, Geography, KU Leuven.

1027 van Vuuren, D.P., Den Elzen, M.G.J., Lucas, P.L., Eickhout, B., Strengers, B.J., van  
1028 Ruijven, B., Wonink, S., van Houdt, R., 2007a. Stabilizing greenhouse gas  
1029 concentrations at low levels: an assessment of reduction strategies and costs.  
1030 *Clim. Change*. 81,119–159.

1031 van Vuuren, D.P., Edmonds, J., Kainuma, M.L.T., Riahi, K., Thomson, A., Matsui, T.,  
1032 Hurtt, G., Lamarque, J-F., Meinshausen, M., Smith, S., Grainer, C., Rose, S.,  
1033 Hibbard, K.A., Nakicenovic, N., Krey, V., Kram, T., 2011. Representative  
1034 concentration pathways: An overview. *Clim. Change*. 109, 5-31.

1035 vanVuuren, D.P., Eickhout, B., Lucas, P.L., den Elzen, M.G.J., 2006. Long-termmulti-  
1036 gas scenarios to stabilise radiative forcing - exploring costs and benefits within an  
1037 integrated assessment framework. *Energ J.* 27, 201–233.

1038 Verstraeten, G., Poesen, J., Goossens, D., Gillijns, K., Bielders, C., Gabriels, D.,  
1039 Ruysschaert, G., van den Eeckhaut, M., Vanwalleghem, T., Govers, G., 2006.  
1040 Belgium, in: Boardman, J., Poesen, J. (Eds.), *Soil Erosion in Europe*. Wiley,  
1041 Chichester, pp. 384-411.

1042 Verstraeten, G., Poesen, J., Govers, G., Gillijns, K., van Rompaey, A., van Oost, K.,  
1043 2003. Integrating science, policy and farmers to reduce soil loss and sediment  
1044 delivery in Flanders, Belgium. *Env. Sci. Policy*. 6, 95-103.

1045 Watanabe, S., et al., 2011. MIROC-ESM 2010: model description and basic results of  
1046 CMIP5-20c3m experiments. *Geosci. Mod. Dev.* 4 (4), 845-872.

1047 Wilby, R.L. Dessai, S., 2010. Robust adaptation to climate change. *Weather*. 65 (7),  
1048 180-185.

1049 Wise, M., Calvin, K., Thomson, A., Clarke, L., Bond-Lamberty, B., Sands, R., Smith,  
1050 S.J., Janetos, A., Edmonds, J., 2009. Implications of limiting CO<sub>2</sub> concentrations  
1051 for land use and energy. *Science*. 324, 1183–1186.

1052 World Reference Base (1998) World Reference Base for soil resources. World  
1053 Resources Report, vol. 84, FAO, Rome, Italy.

1054 Yu, B., 2003. An assessment of uncalibrated CLIGEN in Australia. *Agric. Meteorol.*  
1055 119, 131-148.

1056 Zhang, J.X., Chang, K-T., Wu, J.Q., 2008. Effects of DEM resolution and source on  
1057 soil erosion modelling: a case study using the WEPP model. *International Journal*  
1058 *of Geographical Information Science*. 22 (8), 925-942.

1059 Zhang, W.H., Montgomery, D.R., 1994. Digital elevation model grid size, landscape  
1060 representation, and hydrologic simulations. *Water Resources Research*. 30, 1019-  
1061 1028.

1062 Zhang, X.C., 2007. A comparison of explicit and implicit spatial downscaling of GCM  
1063 output for soil erosion and crop production assessments. *Clim. Change*. 84, 337-  
1064 363.

1065 Zhang, X.C., 2016. Adjusting skewness and maximum 0.5 hour intensity in CLIGEN  
1066 to improve extreme event and sub-daily intensity generation for assessing climate  
1067 change impacts. *Transactions of the ASABE*. 56 (5), 1703-1713.

1068 Zhang, X.C., 2005. Spatial downscaling of global climate model output for site-specific  
1069 assessment of crop production and soil erosion. *Agric. For. Meteorol.* 135, 215-  
1070 229.

1071 Zhang, X-C., 2013. Verifying a temporal disaggregation method for generating daily  
1072 precipitation of potentially non-stationary climate change for site-specific impact  
1073 assessment. *Int. J. Climatol.* 33, 326-342.

1074 Zhang, X-C., Chen, J., Garbrecht, J.D., Brissette, F.P., 2012. Evaluation of a weather  
1075 generator-based method for statistically downscaling non-stationary climate  
1076 scenarios for impact assessment at a point scale. *Transactions of the ASABE*. 55  
1077 (5), 1 – 12.

1078 Zhang, X.C., Liu, W.Z., 2005. Simulating potential response of hydrology, soil erosion,  
1079 and crop productivity to climate change in Changwu tableland region on the Loess  
1080 Plateau of China. *Agric. For. Meteorol.* 131, 127-142.



1081 Zhang, X.C., Liu, W.Z., Li, Z., Zheng, F.L., 2009. Simulating site-specific impacts of  
1082 climate change on soil erosion and surface hydrology in southern Loess Plateau  
1083 of China. *Catena*. 79 (3), 237-242.

1084 Zhang, X.C., Nearing, M.A., 2005. Impact of climate change on soil erosion, runoff and  
1085 wheat productivity in central Oklahoma. *Catena*. 61, 185-195.

1086 Zhang, X.C., Nearing, M.A., Garbrecht, J.D., Steiner, J.L., 2004. Downscaling monthly  
1087 forecasts to simulate impacts of climate change on soil erosion and wheat  
1088 production. *Soil Sci. Soc. Am. J.* 68, 1376-1385.